

The diagram illustrates a digital PLL system. On the left, a vector diagram shows a circle with eight points. The horizontal axis is labeled 'I' and the vertical axis is labeled 'Q'. The points are at the intersections of the axes and at 45-degree intervals. The top path processes the 'I' input through a 'Sqrt Nyquist Filter', a ' $x/\sin x$ ' block, a 'D/A' converter, and an 'LPF' block. The output is then multiplied by  $\cos 2\pi f_c t$ . The bottom path processes the 'Q' input through the same sequence of blocks. The output is then multiplied by  $\sin 2\pi f_c t$ . The final outputs of these two multiplication blocks are combined to produce the PLL output.

Figure 1A A simplified PSK transmitter.

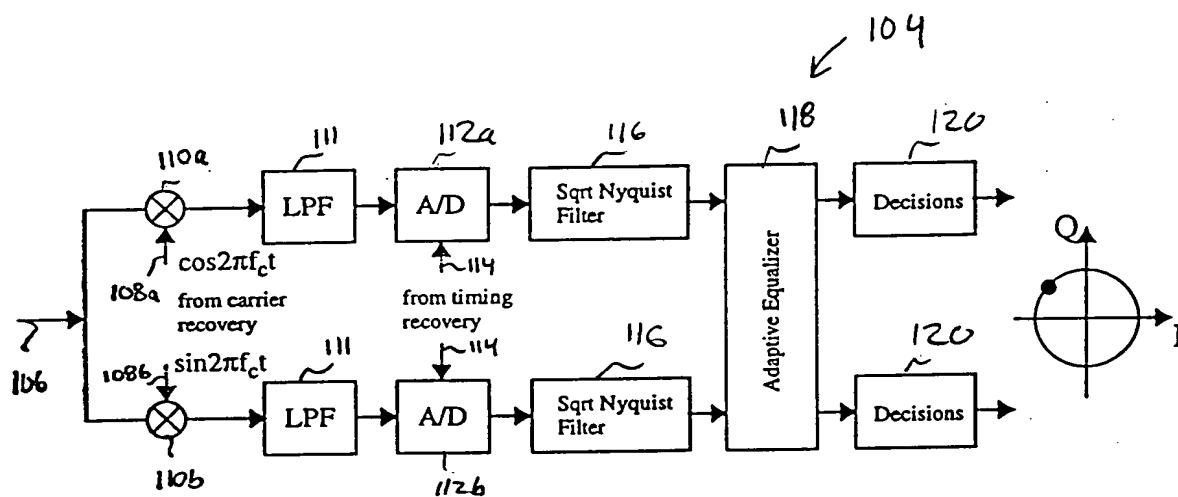


Figure 13 A simplified PSK receiver.

09698246 103000

126

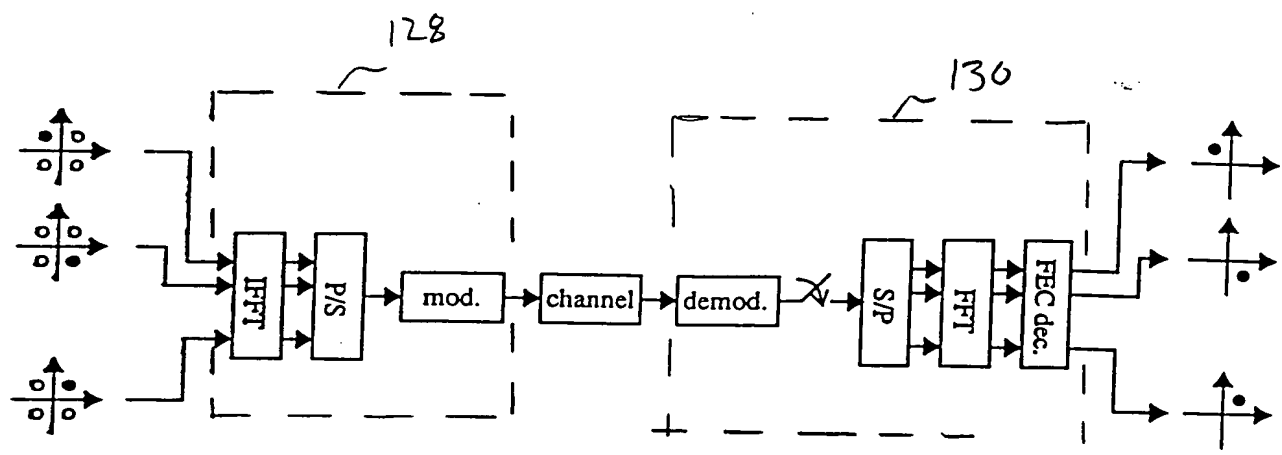


Figure 1C Simplified block diagram of an OFDM system.

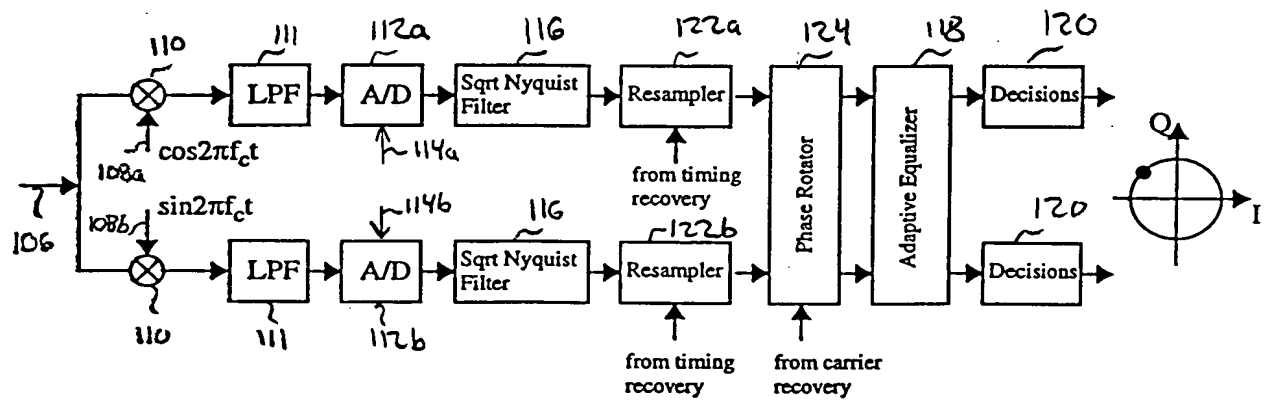


Figure 1D PSK receiver with carrier and timing recovery.

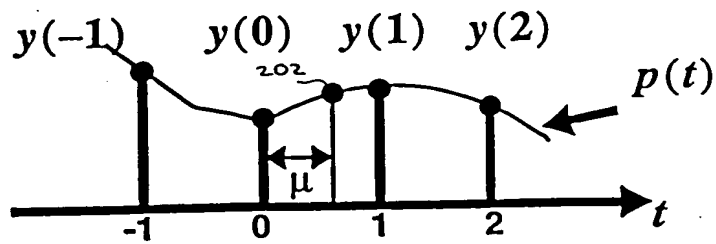
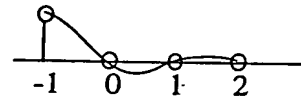
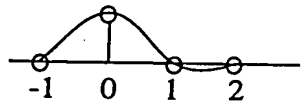


Figure 2 Interpolation Environment

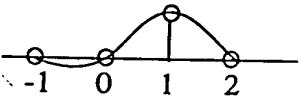
Figure 1 consists of 11 small graphs, each showing the relationship between a specific variable and the number of children (0 to 10). The variables are: (a) Age of mother at birth, (b) Age of mother at first birth, (c) Age of mother at last birth, (d) Age of mother at death, (e) Age of mother at marriage, (f) Age of mother at divorce, (g) Age of mother at remarriage, (h) Age of mother at remarriage, (i) Age of mother at remarriage, (j) Age of mother at remarriage, (k) Age of mother at remarriage. Each graph has 'Number of children' on the x-axis (0 to 10) and a y-axis representing the variable. The graphs show different trends for each variable, with some showing a peak and others showing a steady increase or decrease.



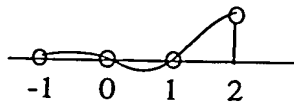
$$C_{-1}(\mu) = -\frac{1}{6}\mu^3 + \frac{1}{2}\mu^2 - \frac{1}{3}\mu$$



$$C_0(\mu) = \frac{1}{2}\mu^3 - \mu^2 - \frac{1}{2}\mu + 1$$



$$C_1(\mu) = \frac{1}{2}\omega^3 + \frac{1}{2}\mu^2 + \mu$$



$$C_2(\mu) = \frac{1}{6}\mu^3 - \frac{1}{6}\mu$$

Figure 3 The Lagrange basis polynomials.



500  
↓

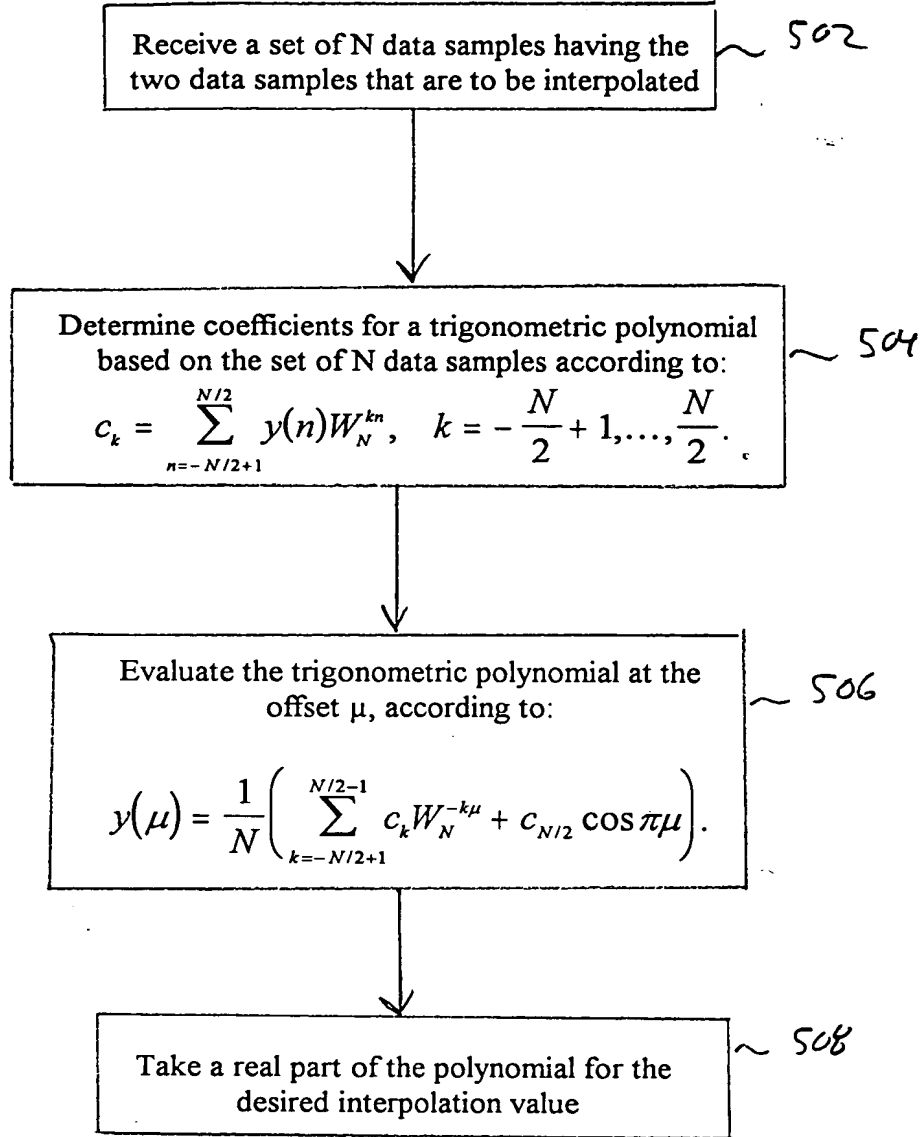


FIG. 5

FIG. 6A

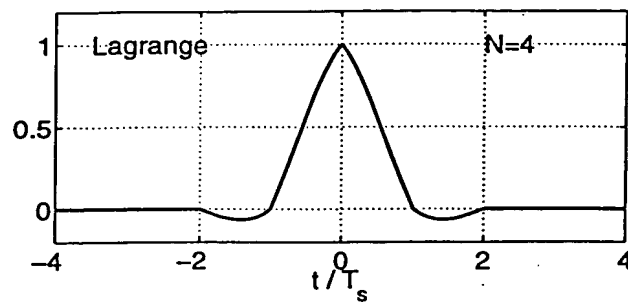


FIG. 6B

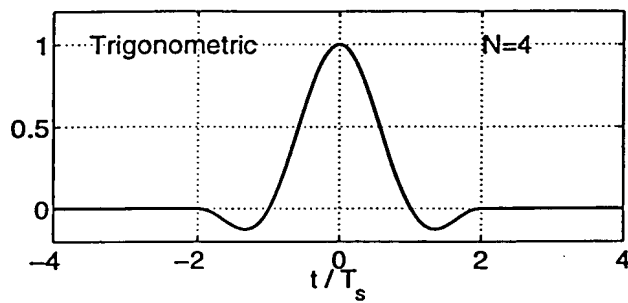


FIG. 6A-6B Impulse responses of (a) Lagrange interpolator and (b) Trigonometric interpolator.

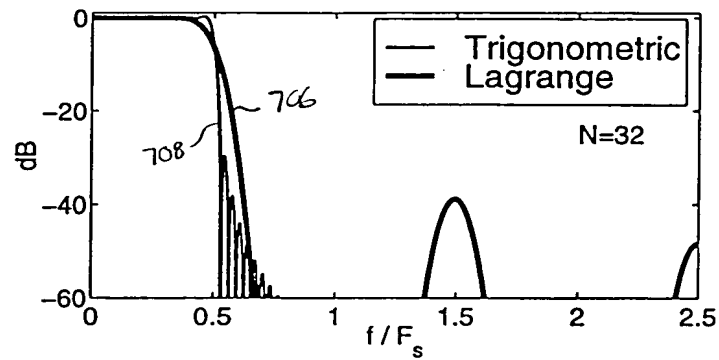
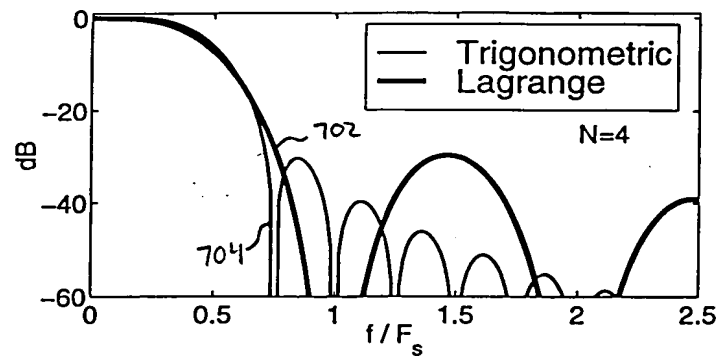


FIG. 7A-7B: Frequency responses for (a)  $N=4$  and (b)  $N=32$ .



N	Lagrange Interpolator (NMSE in dB)	New Interpolator (NMSE in dB)
4	-25.5	-28.5
6	-30.0	-34.5
8	-34.0	-38.5
10	-37.5	-42.5

Figure 1 is a plot of the baseband signal spectrum. The vertical axis is labeled 'dB' and ranges from 0 to -60. The horizontal axis is labeled 'normalized frequency' and ranges from 0 to 2.5. The plot shows a main signal centered at 0.5, with two sideband images centered at 1.5 and 2.5. The signal is labeled 'signal' and the images are labeled 'images'.

**Figure 8A** Signal with two samples/symbol and 100% excess BW.

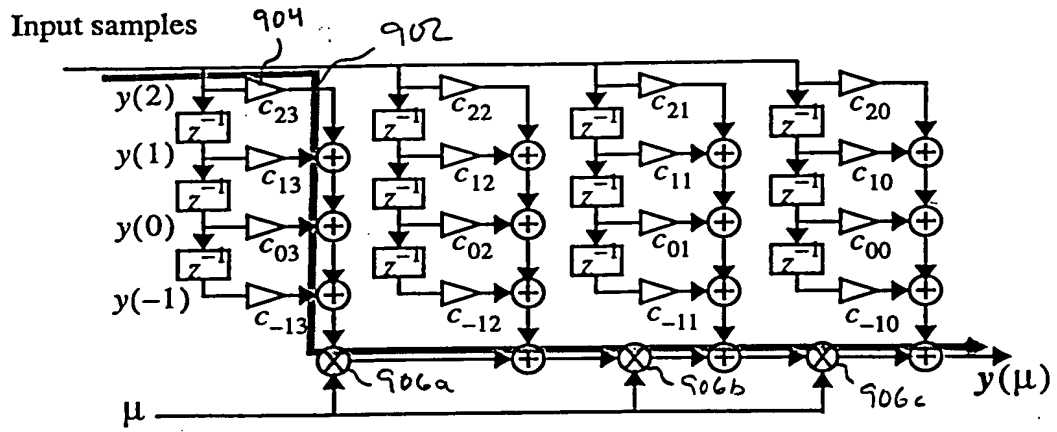


Figure 9 The critical path of the Lagrange cubic interpolator.

1000

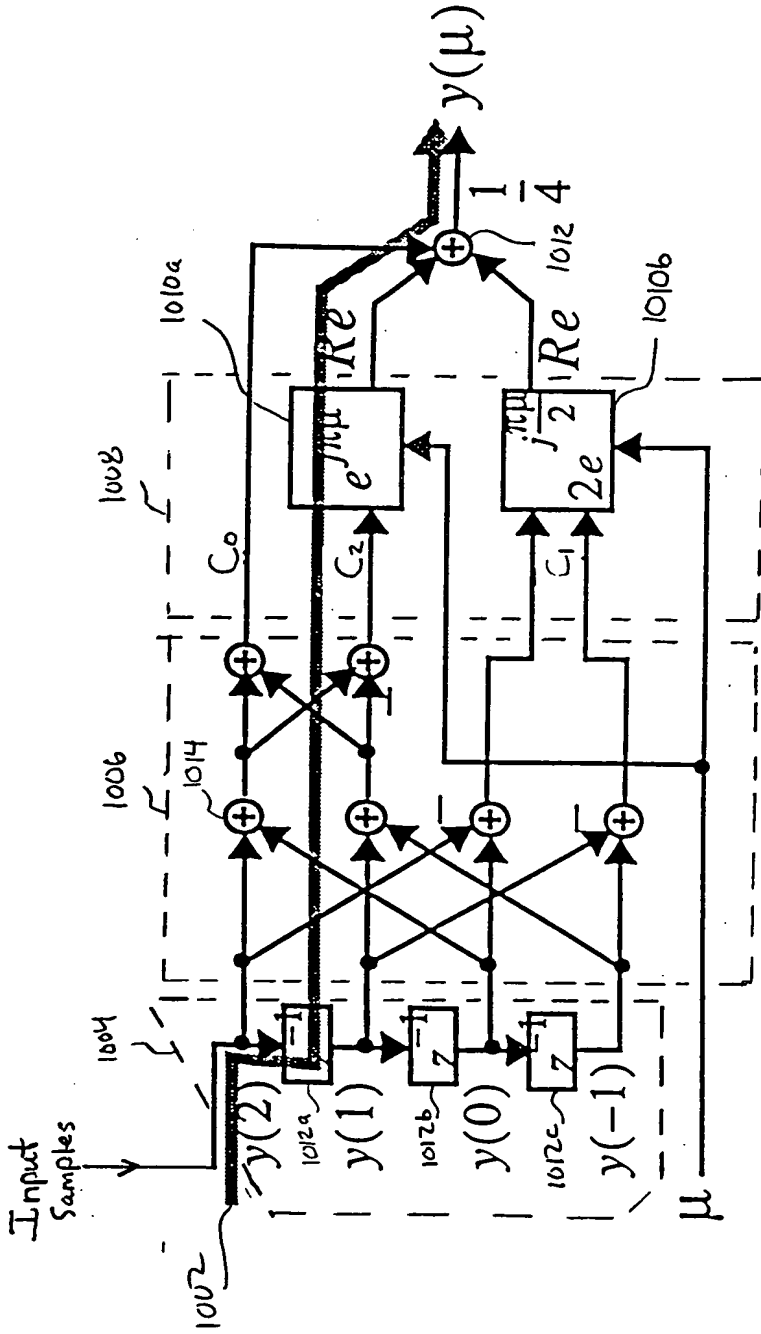


FIG. 10: Trigonometric Interpolator ( $N=4$ )

1100

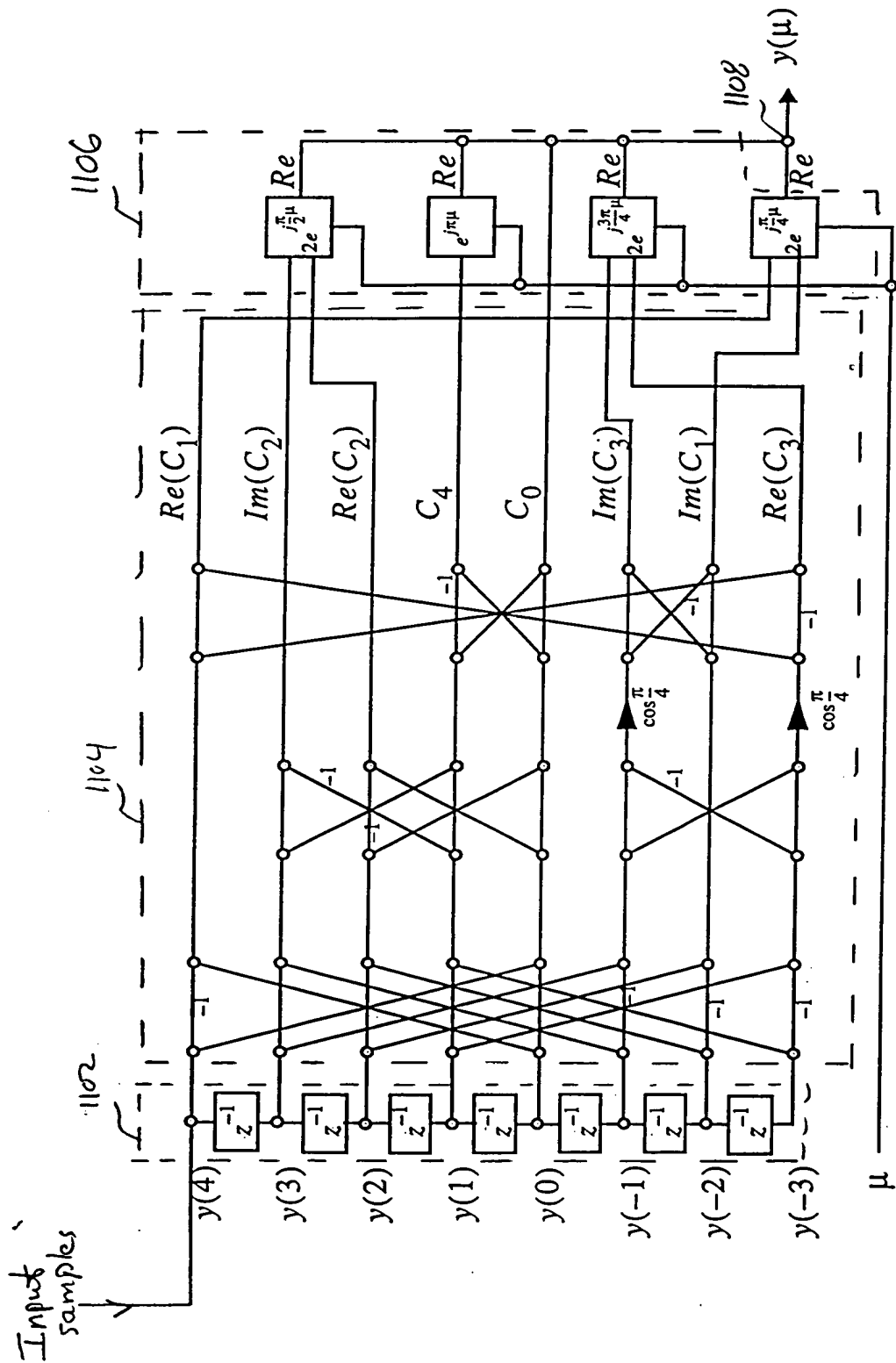


Figure 11 Trigonometric Interpolator with  $N=8$ .

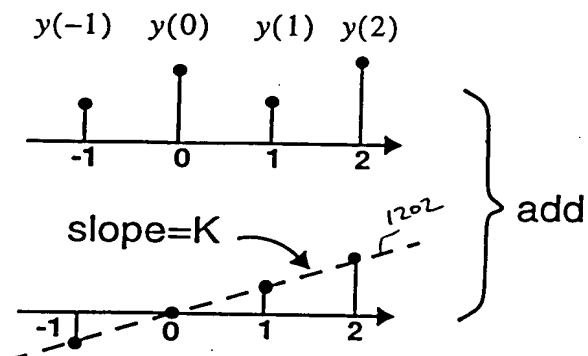


Figure 12 Conceptual modification of input samples.

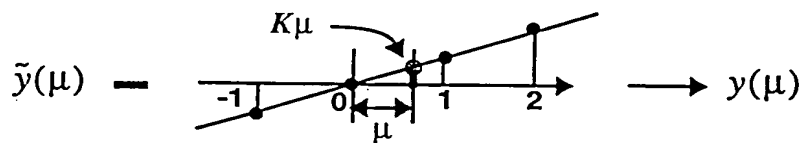


Figure 13 Correcting the offset due to modification of original samples.

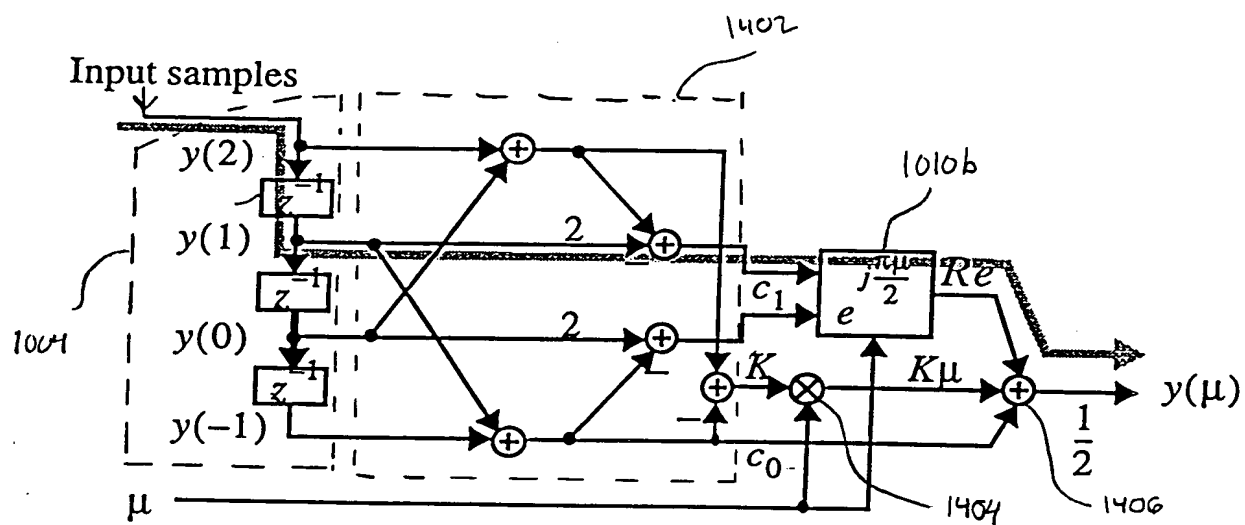


FIG. 14: Trigonometric Interpolator  $N=4$

1500



1506

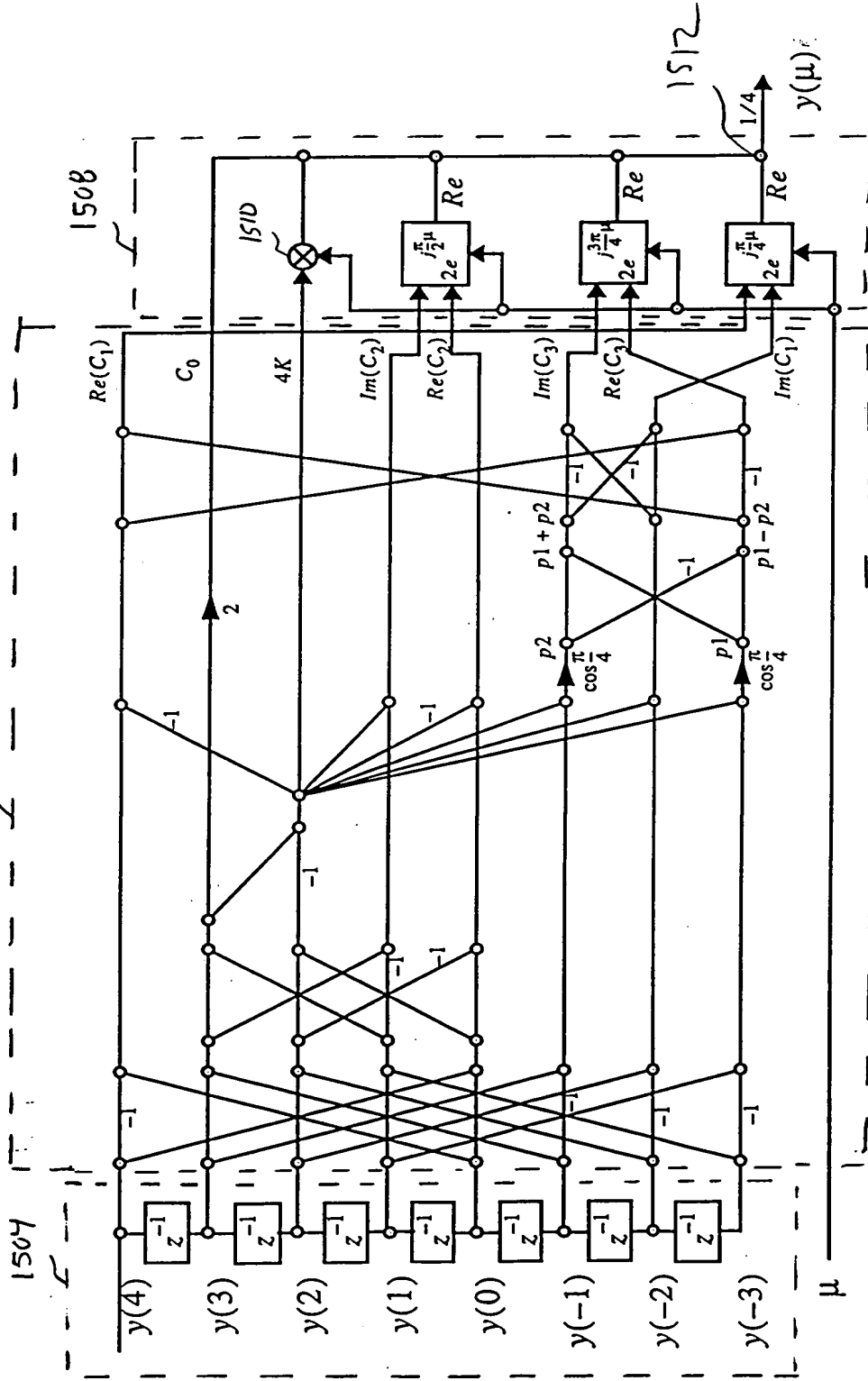
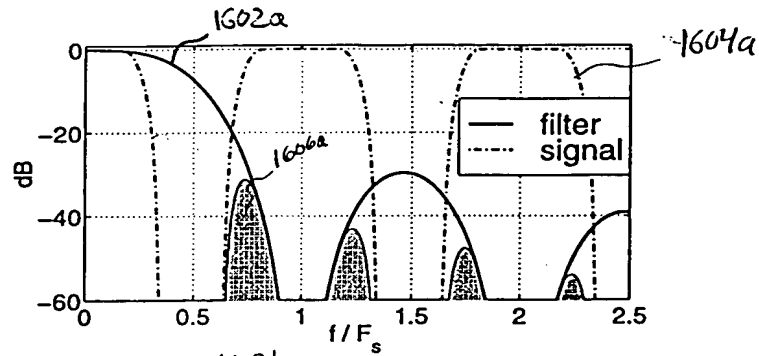


FIG. 15 The modified Trigonometric Interpolator

\_\_\_\_\_

**FIG. 16A: Lagrange cubic**



**FIG. 16B: Trigonometric Interpolator 1000 (FIG. 10)**

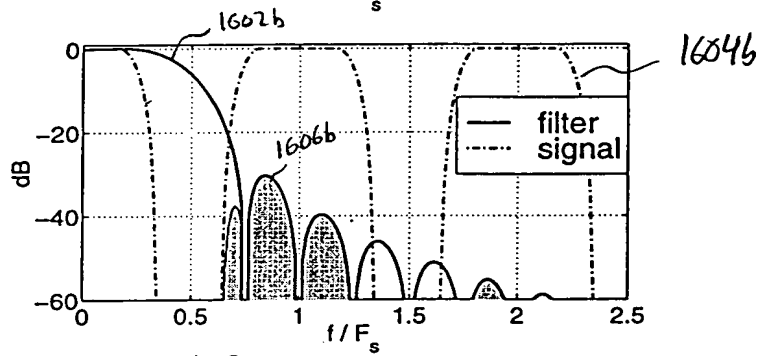
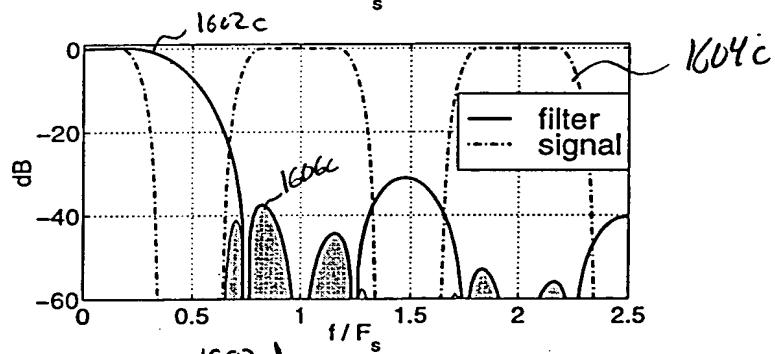
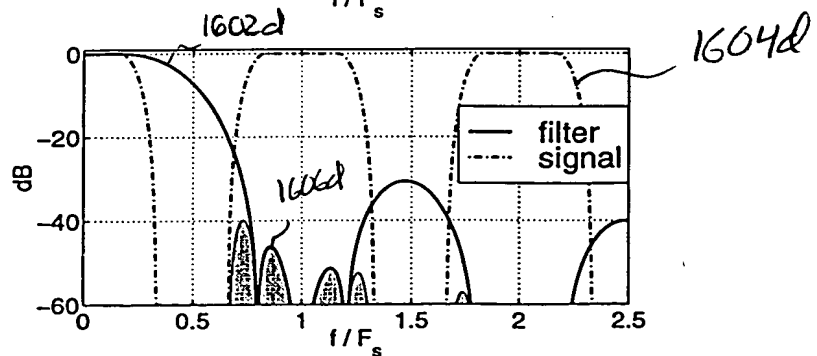


FIG. 16C: Trigonometric Interpolator 1400 (FIG. 14)



**FIG. 16D: Optimal structure**



Variable	Mean	SD	Min	Max
Age	34.5	10.2	22	55
Gender	0.5	0.5	0	1
Marital status	0.6	0.5	0	1
Education	12.5	1.5	10	15
Income	1500	500	1000	2500
Health status	0.8	0.2	0	1
Employment status	0.7	0.3	0	1
Life satisfaction	4.5	1.0	3	6
Depression	0.2	0.4	0	1
Stress	3.5	1.5	2	5
Quality of life	5.5	1.0	4	6
Physical health	0.9	0.1	0	1
Mental health	0.7	0.3	0	1
Social health	0.8	0.2	0	1
Environmental health	0.6	0.4	0	1
Overall health	0.8	0.2	0	1



↓

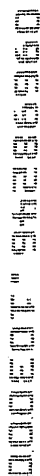
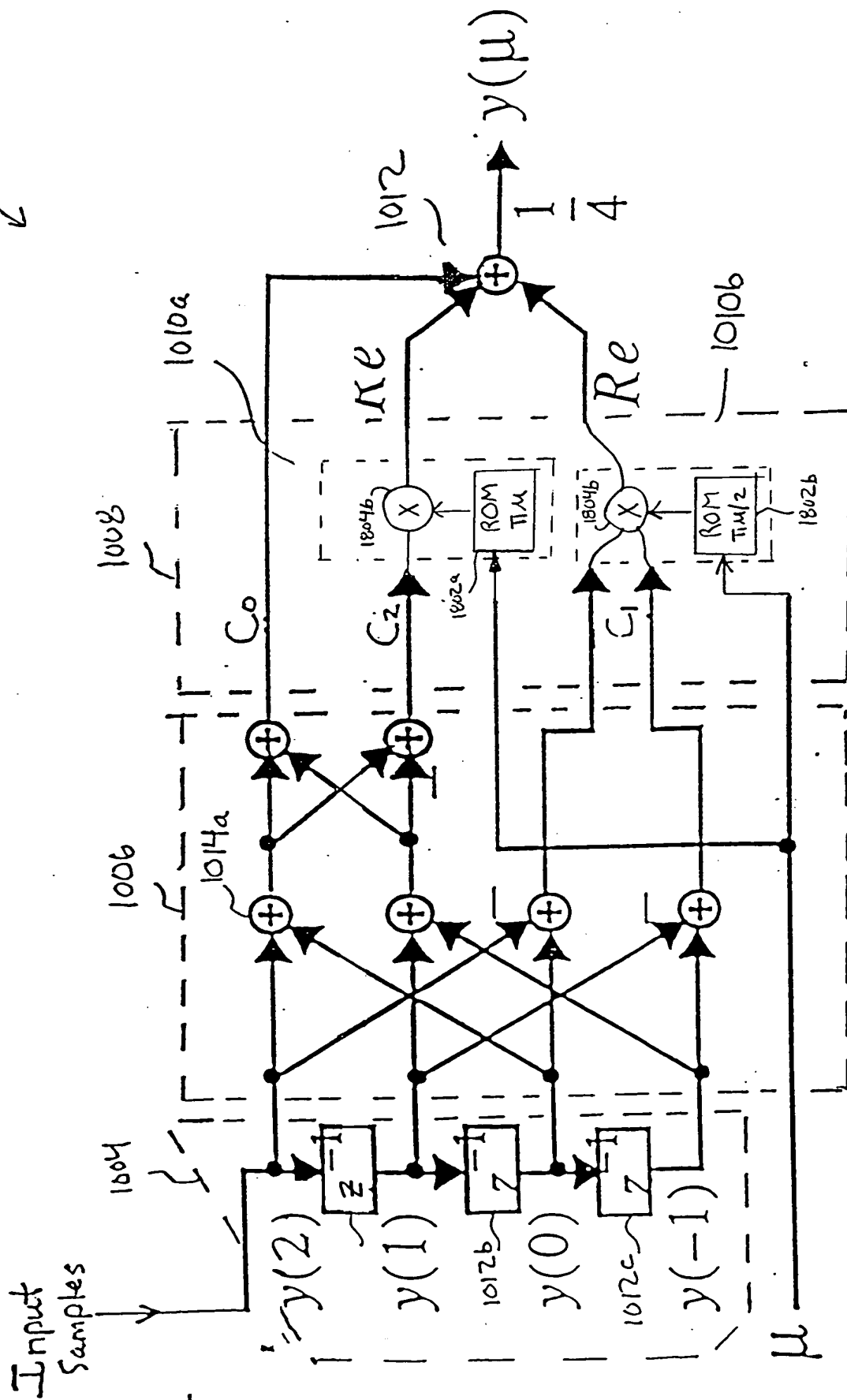


FIG. 17



↓

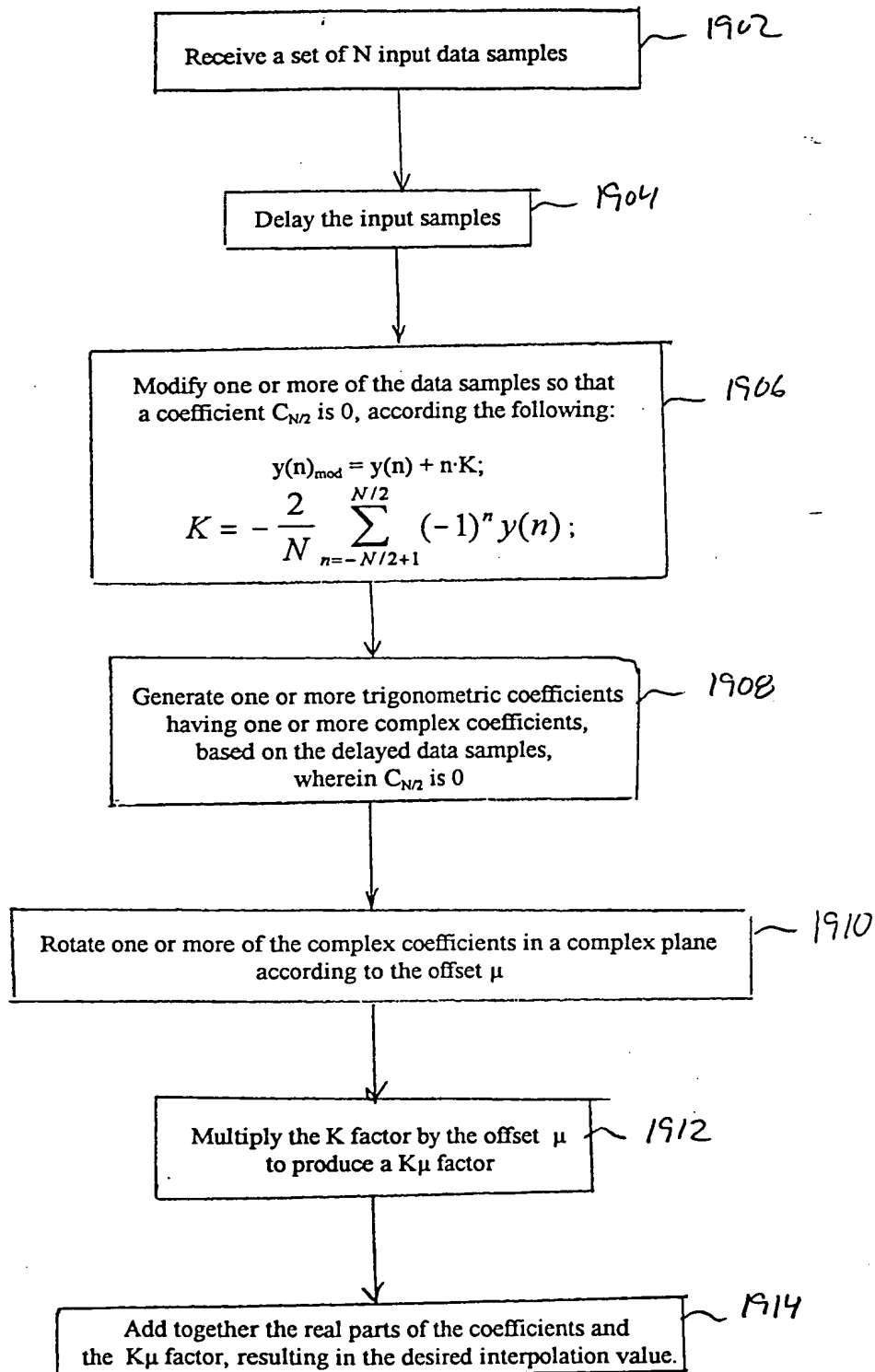


FIG. 19

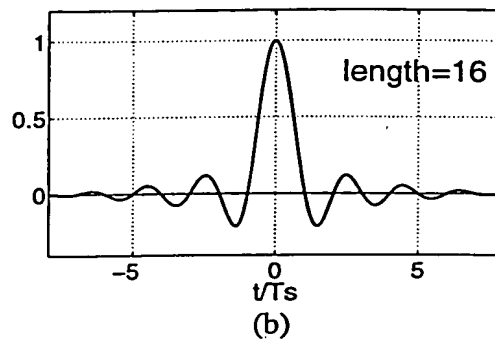
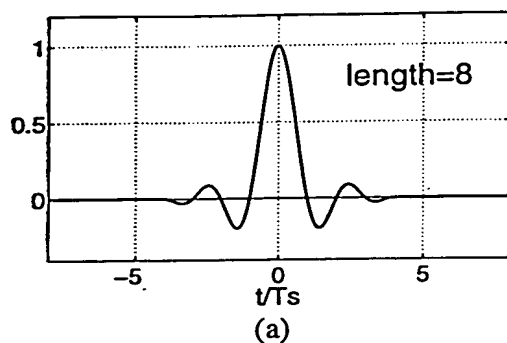


FIG. 20: Normalized Impulse responses  $f$  of the interpolation filters.

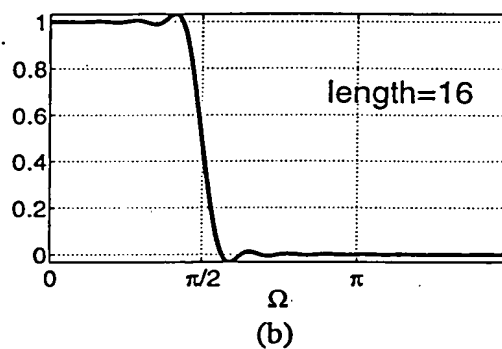
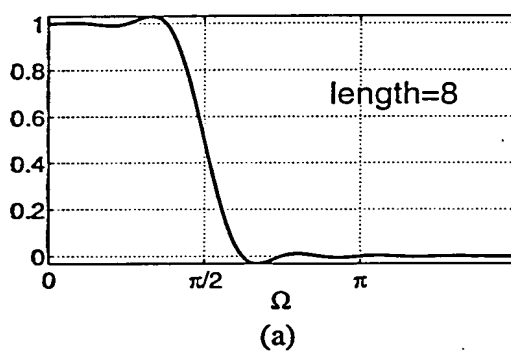


FIG. 21: Normalized Frequency responses  $F$  of the interpolation filters.

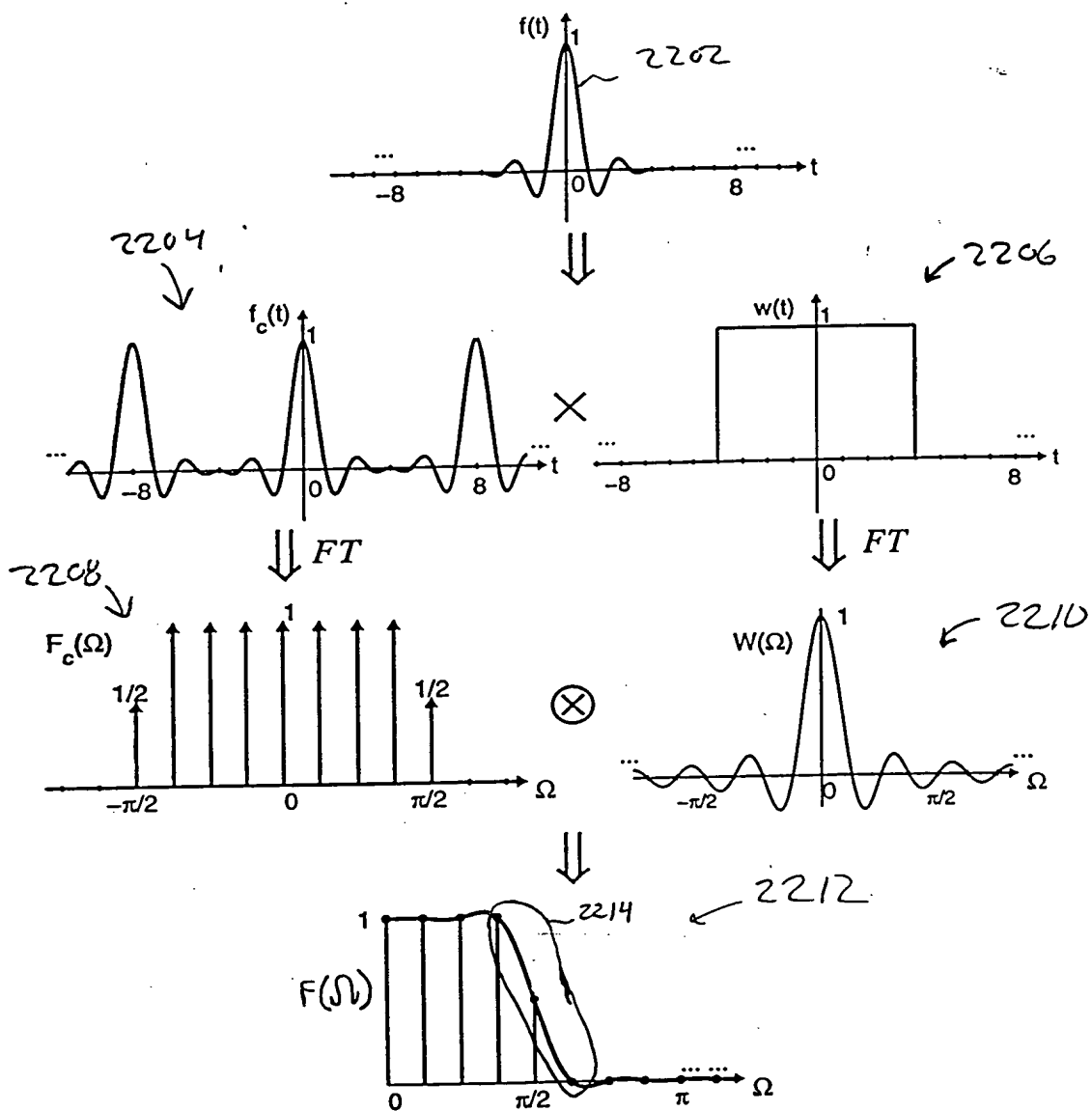


FIG. 22: Analysis of the frequency responses.

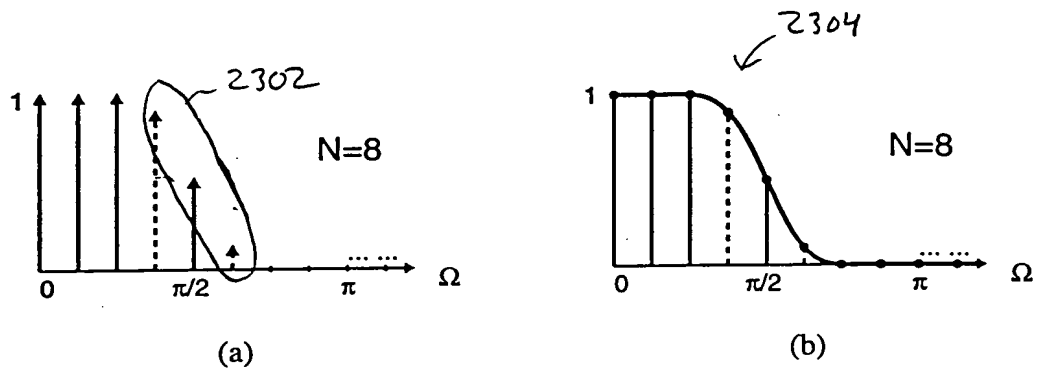


FIG. 23 Effect of a more gradual transition at the band edge.

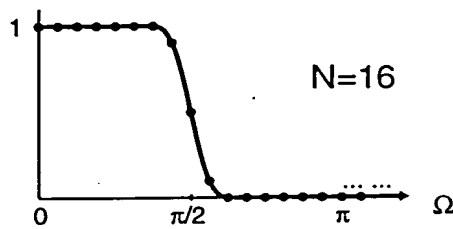


FIG. 24 Reducing the transition bandwidth by increasing  $N$ .

3-4b, in which  $N = 8$ .

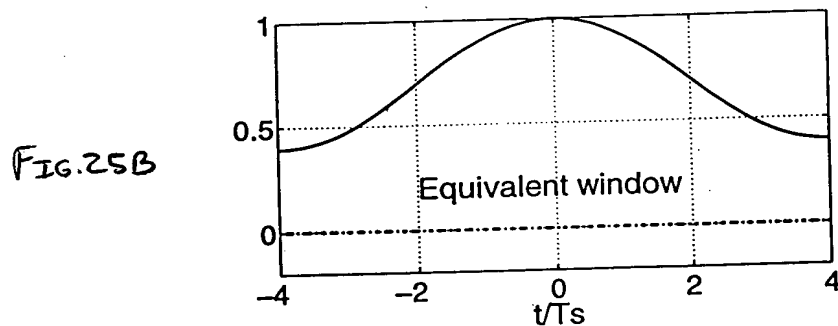
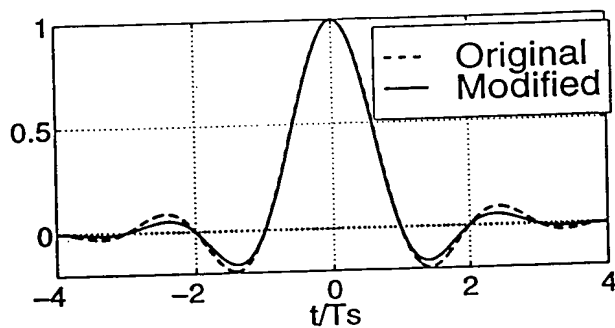


FIG. 25A-B: (A) Impulse response of the original filter and the modified filter: (B) The equivalent window.

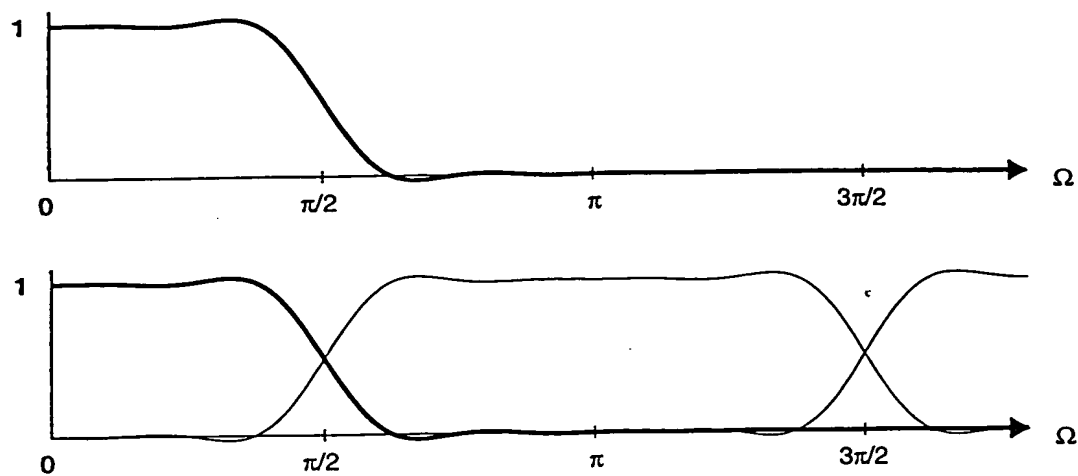


FIG. 26 Forming the frequency response of the discrete-time fractional-delay filter.



FIG. 27A

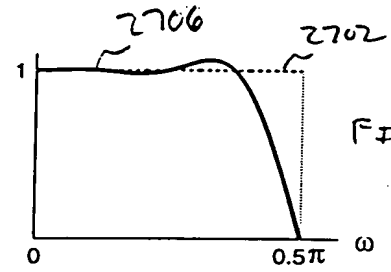
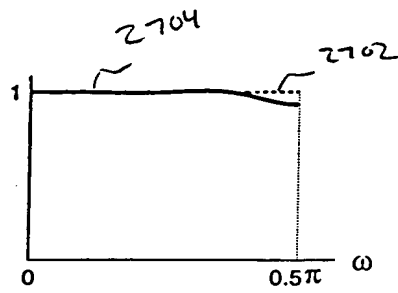


FIG. 27B

FIG. 27A-B: Fractional-delay filter with (A)  $\mu=0.12$  and (B)  $\mu=0.5$ , using the preliminary  $N=8$  interpolator.

000001" 94886960

FIG. 28A

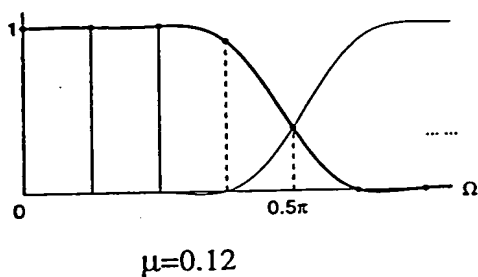


FIG. 28B

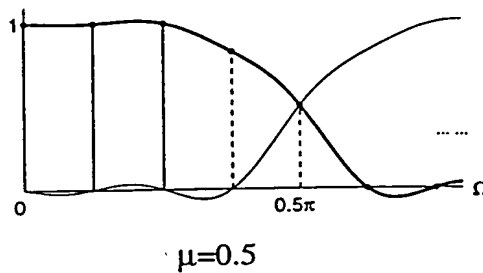


FIG. 28C

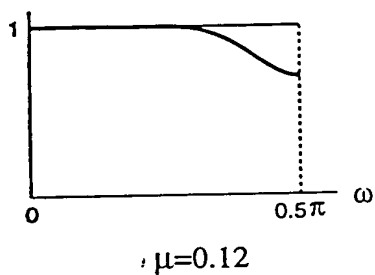
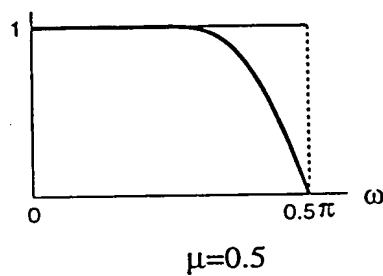


FIG. 28D



000001 94286960

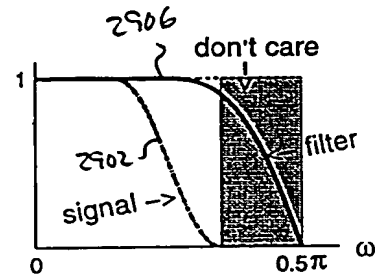
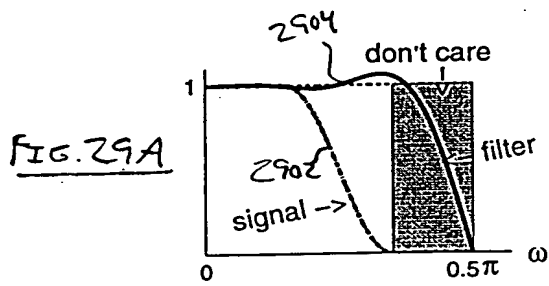


FIG. 29A-B :  $F_\mu(\omega)$ , with  $\mu=0.5$ ,  $N=8$ , (A) before and (B) after optimization.

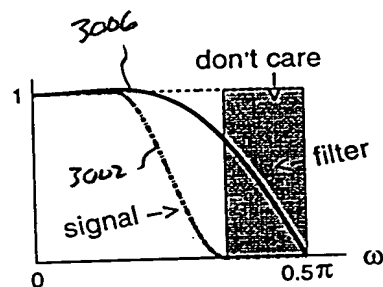
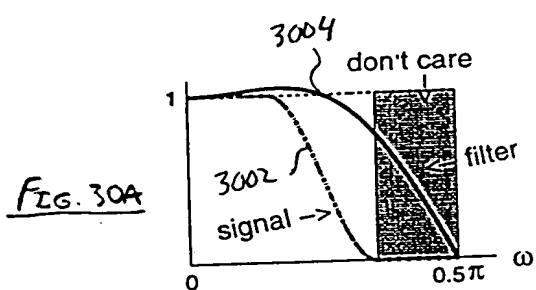


FIG. 30B

FIG. 30A-B  $F_{\mu}(\omega)$  for  $\mu=0.5$ ,  $N=4$ , A) before and B) after modification.

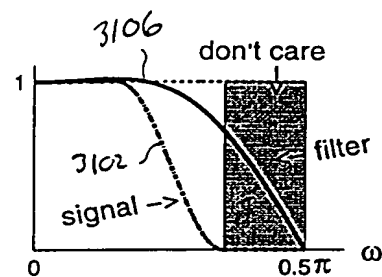
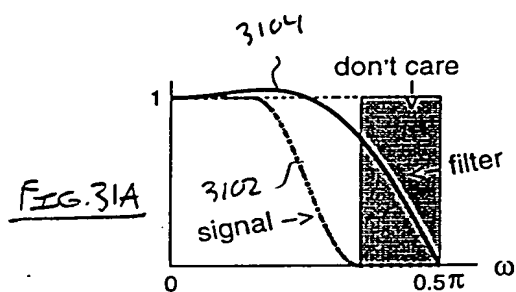


FIG. 31A-B  $F_{\mu}(\omega)$ ,  $\mu=0.5$ , simplified  $N=4$  structure, A: before and B: after modification.

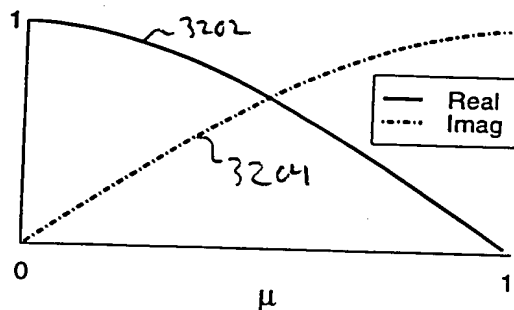


FIG. 32: Real and imaginary components of the  $f_{\mu}(1)e^{j\frac{\pi}{2}\mu}$  value.

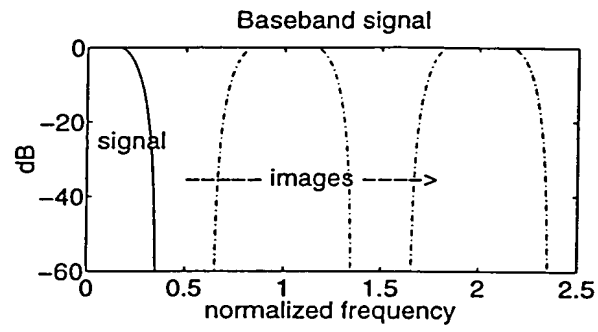


FIG.33: Signal with two samples/symbol and 40% excess bandwidth.

09698246-103000

3400  
↓

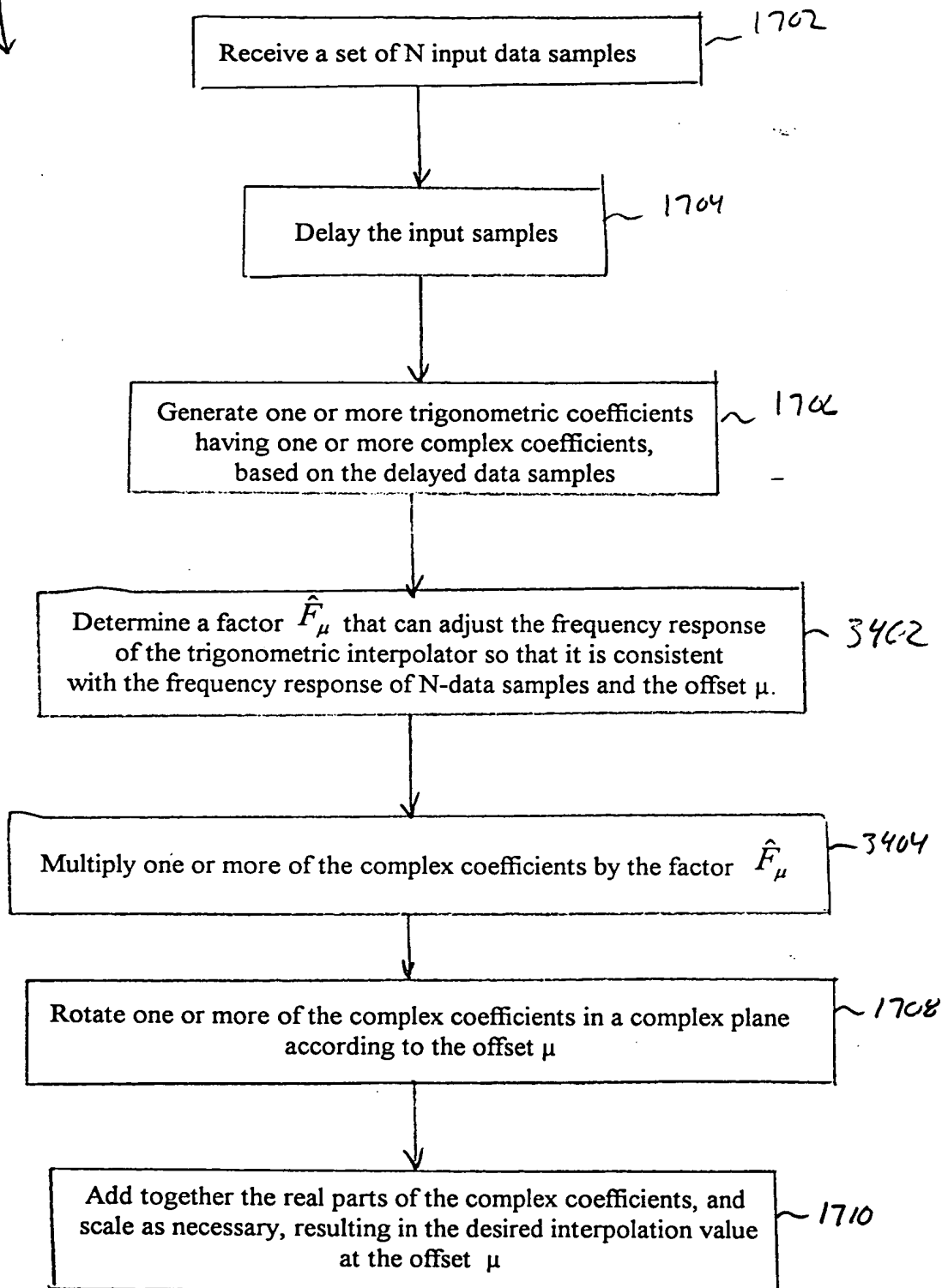


FIG. 34



3500  
↓

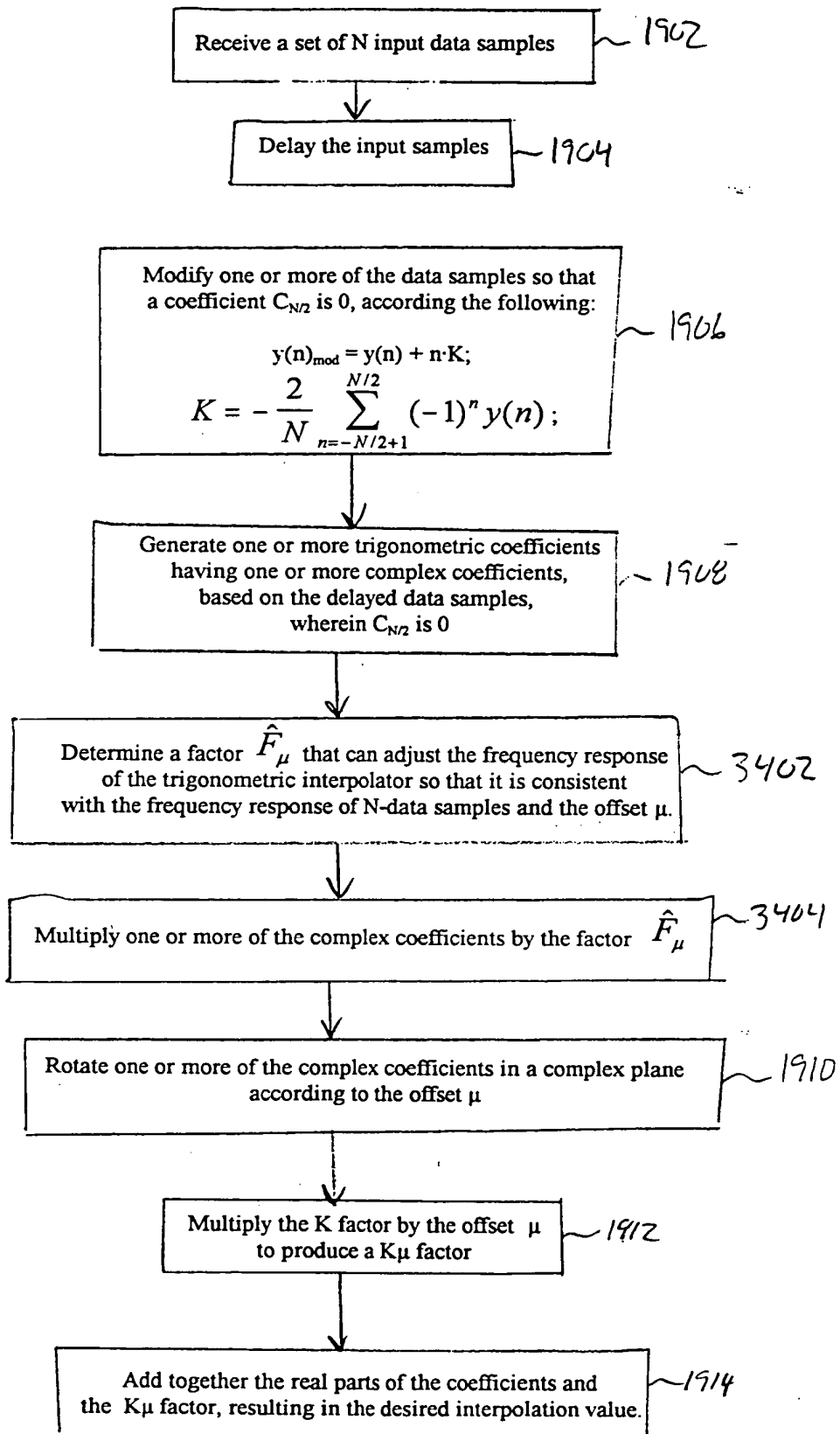


FIG. 35

3600

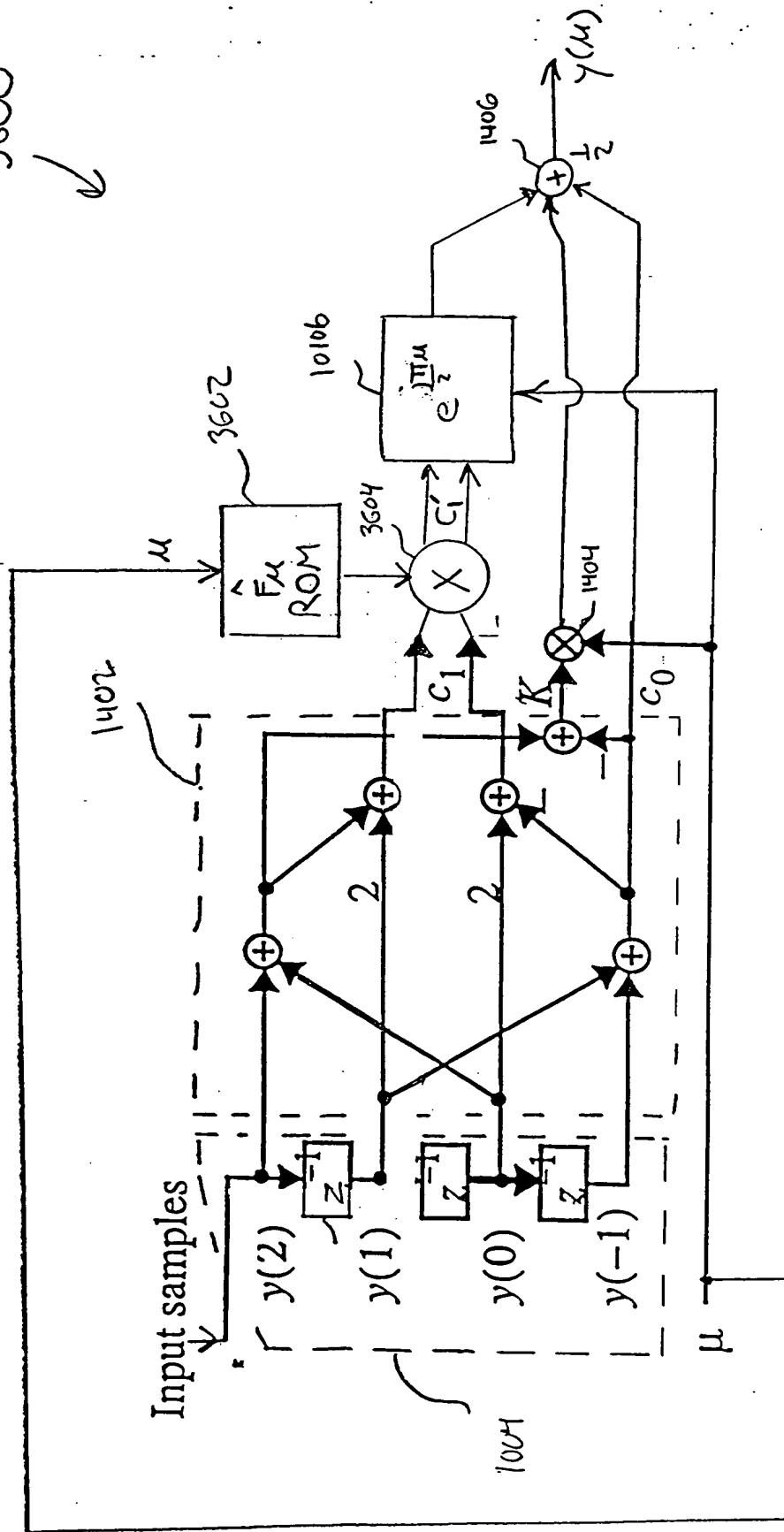


FIG. 36 The optimized structure for  $N=4$ .

3700

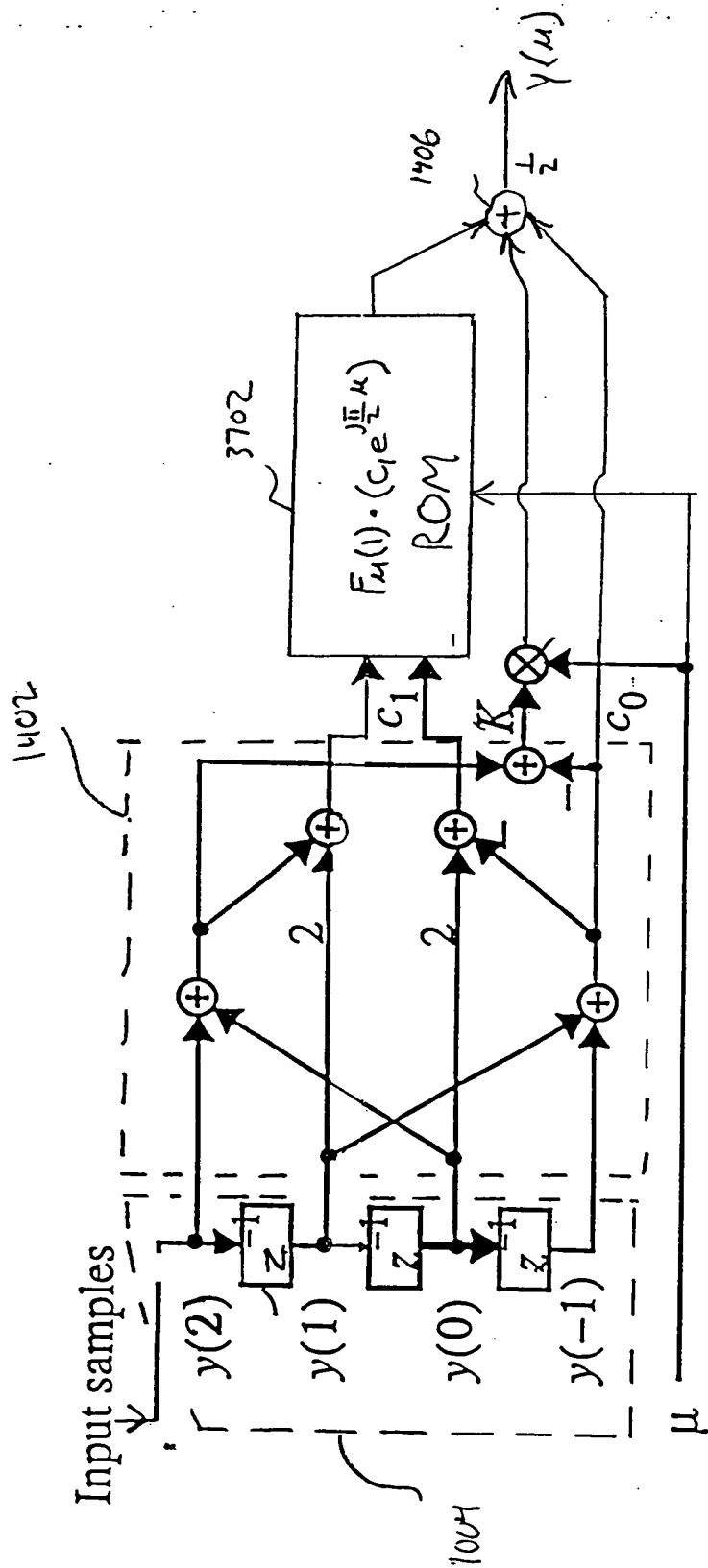


FIG. 37 : The optimized structure for  $N=4$ .

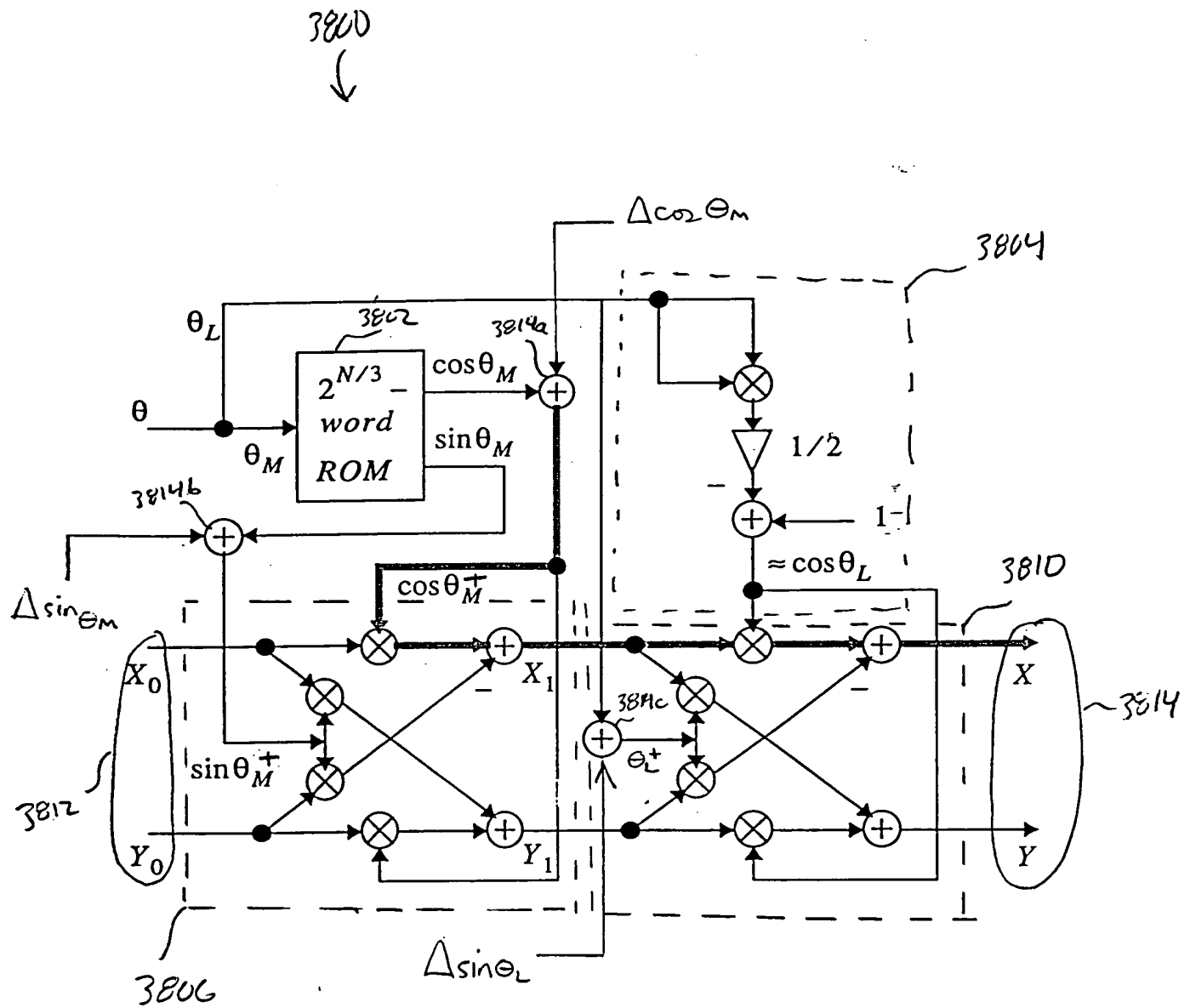


FIG. 38

3906

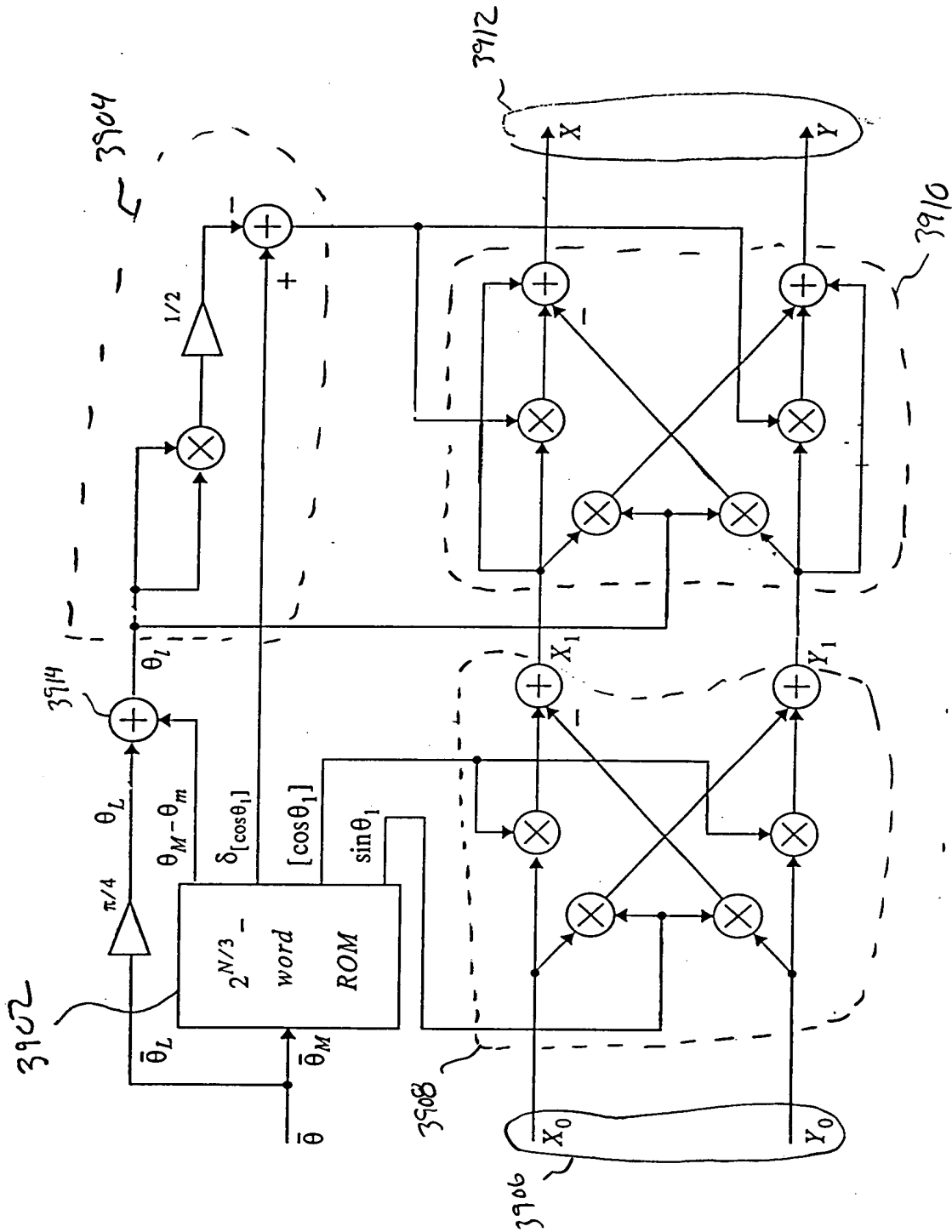
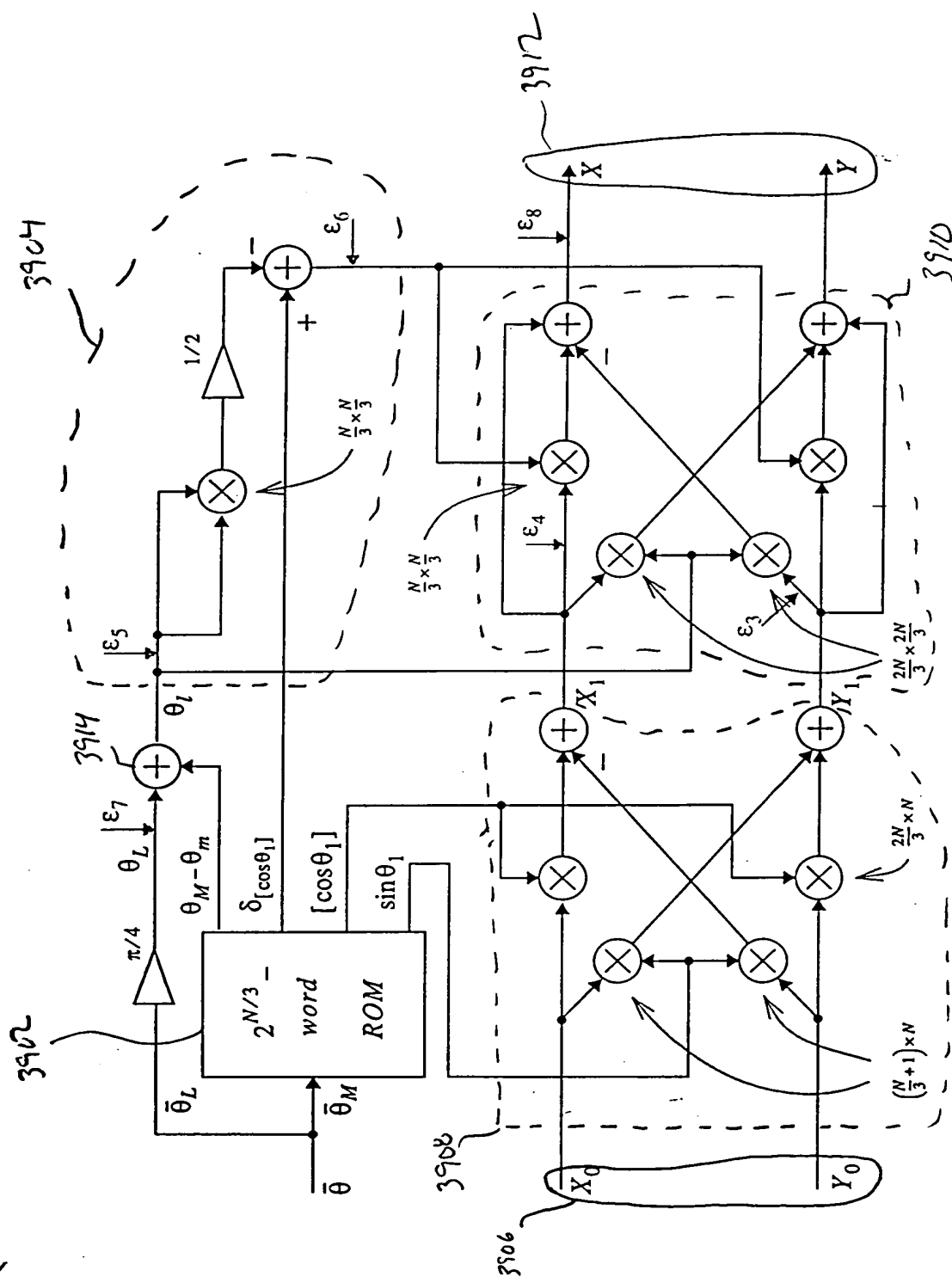


FIG. 39



4100  
↓

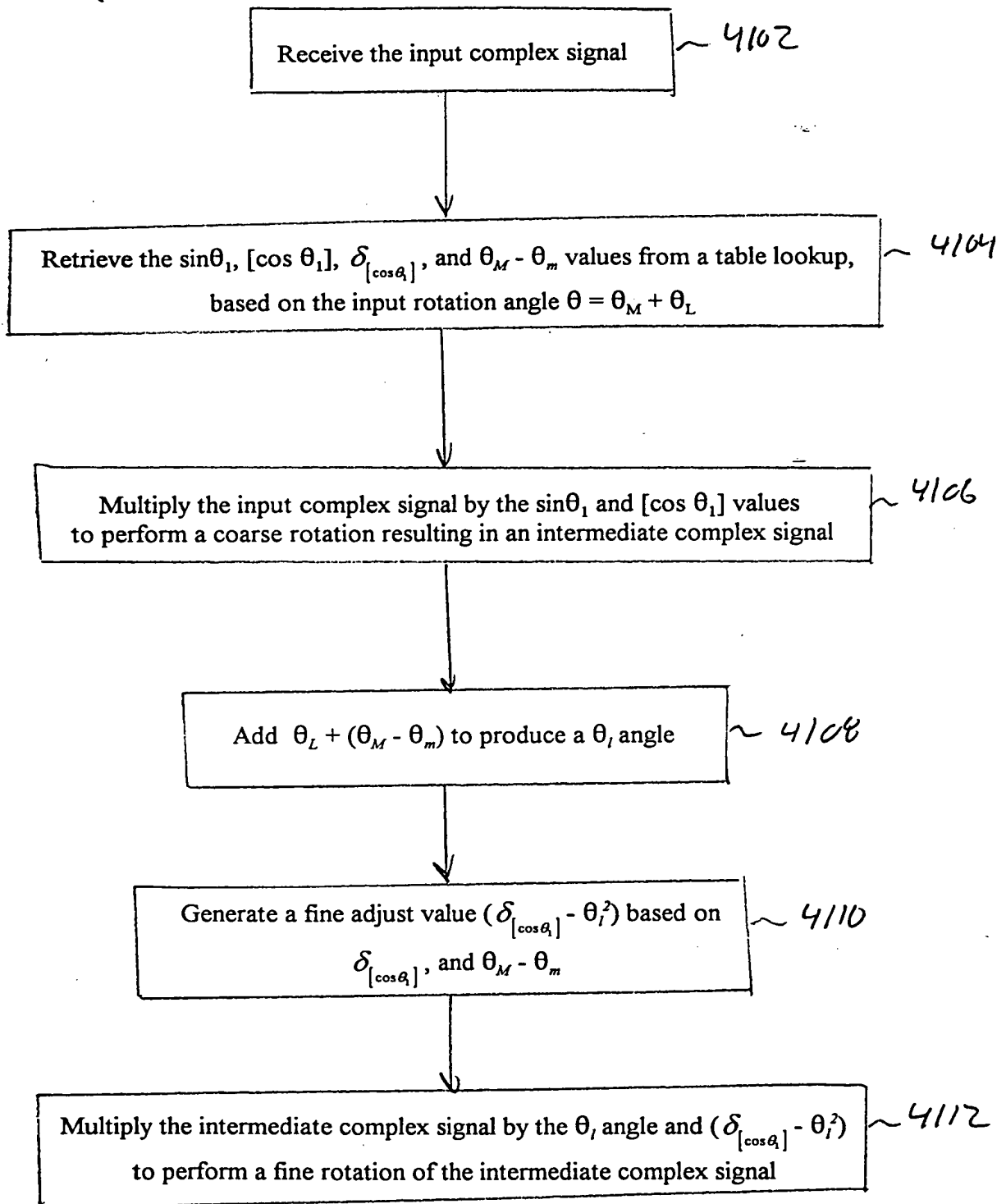


FIG. 41

3900  
↓

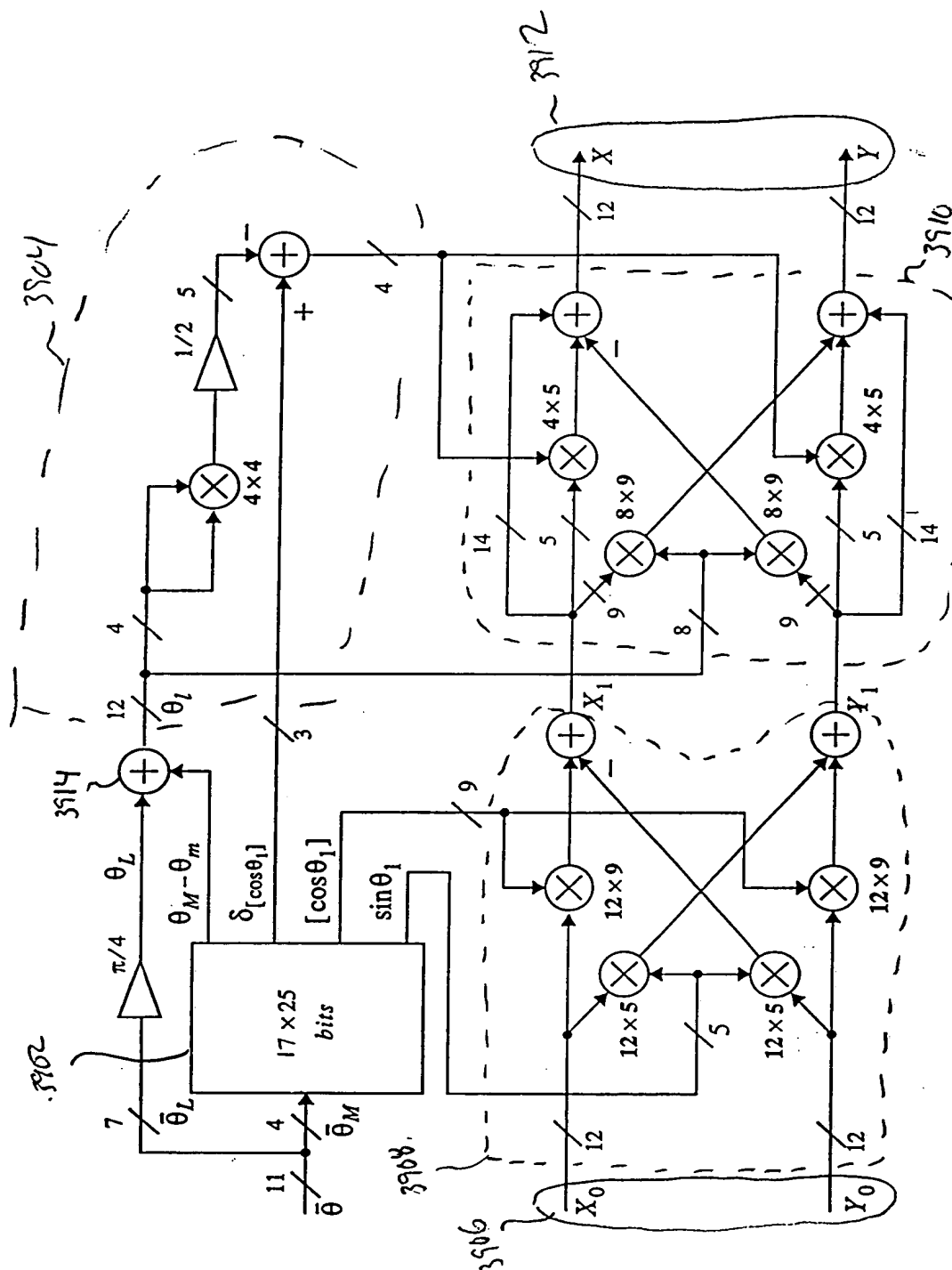


FIG. 42 The internal wordlength of the structure that achieved 90.36 dB SFDR.



FIG. 43 Output spectrum showing 90.36 dB SFDR.

4406

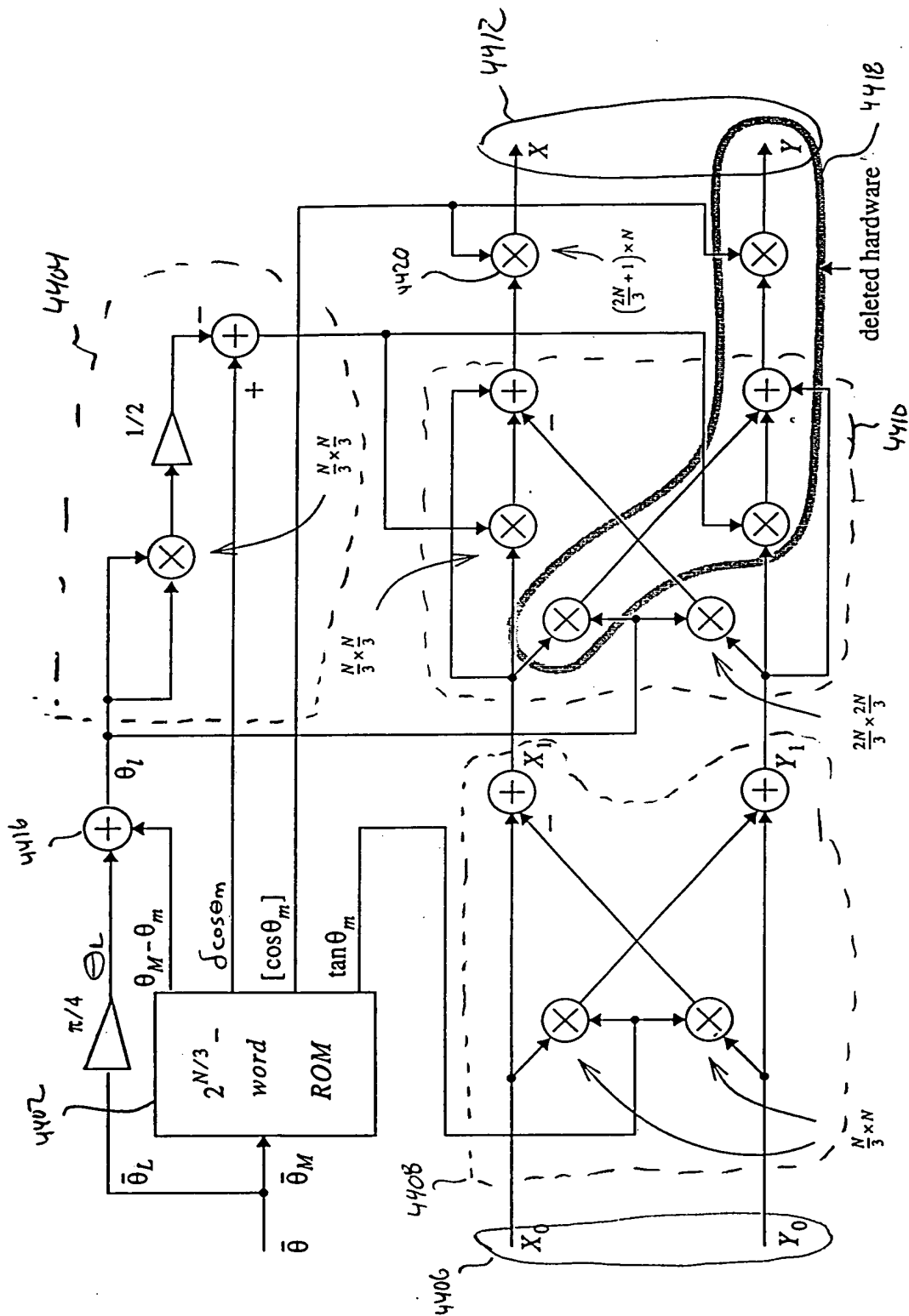
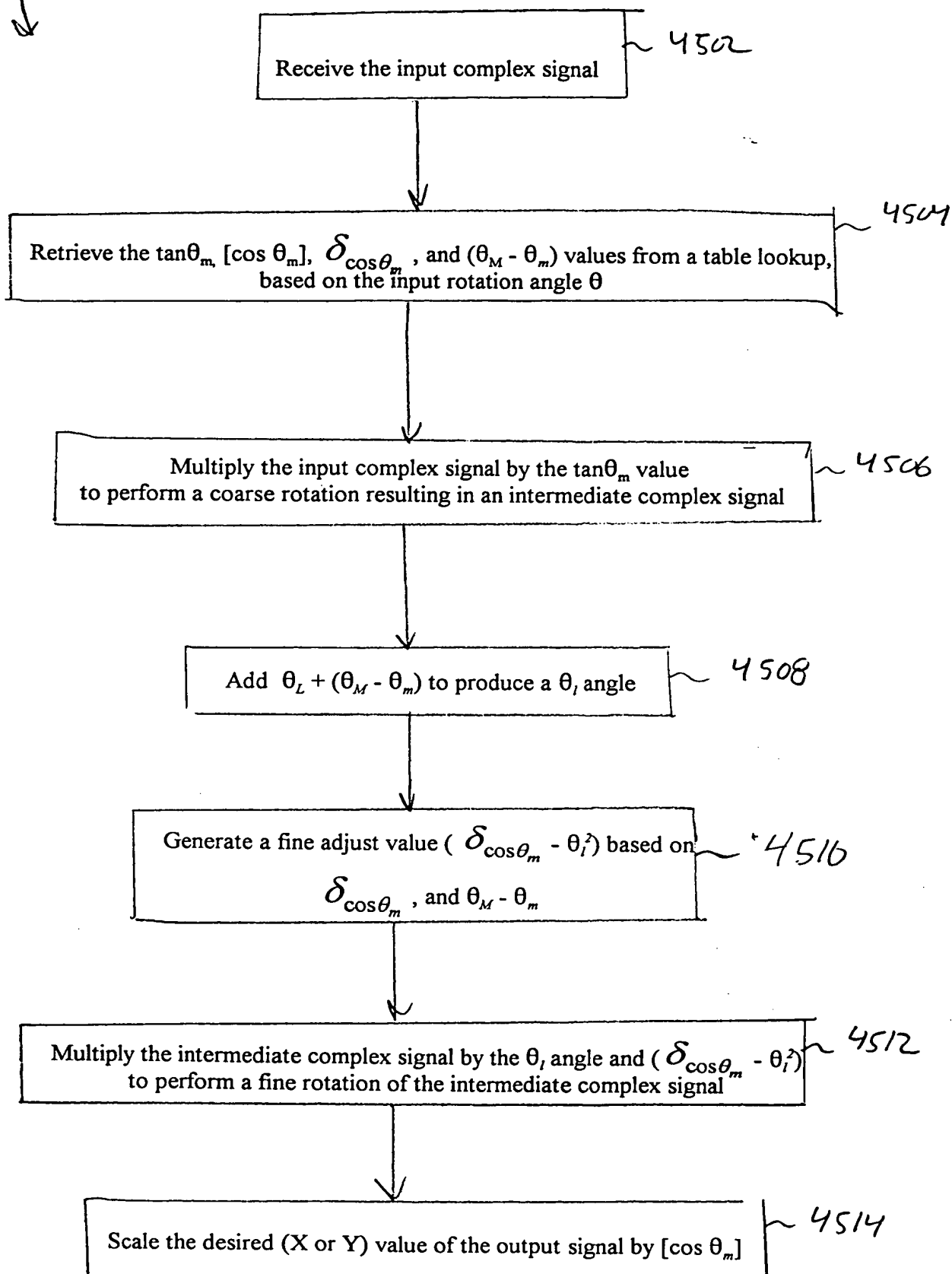


FIG. 44 A modified architecture when only one output is needed.

↓



4600

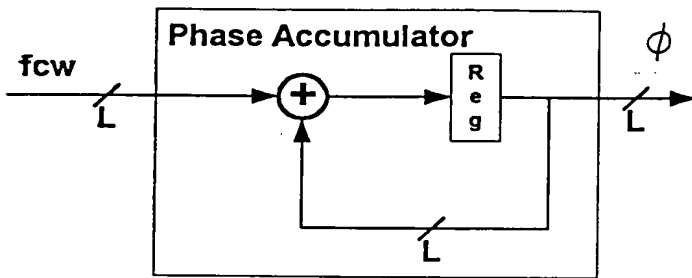


FIG. 46

where the adder is an overflowing accumulator.

4700

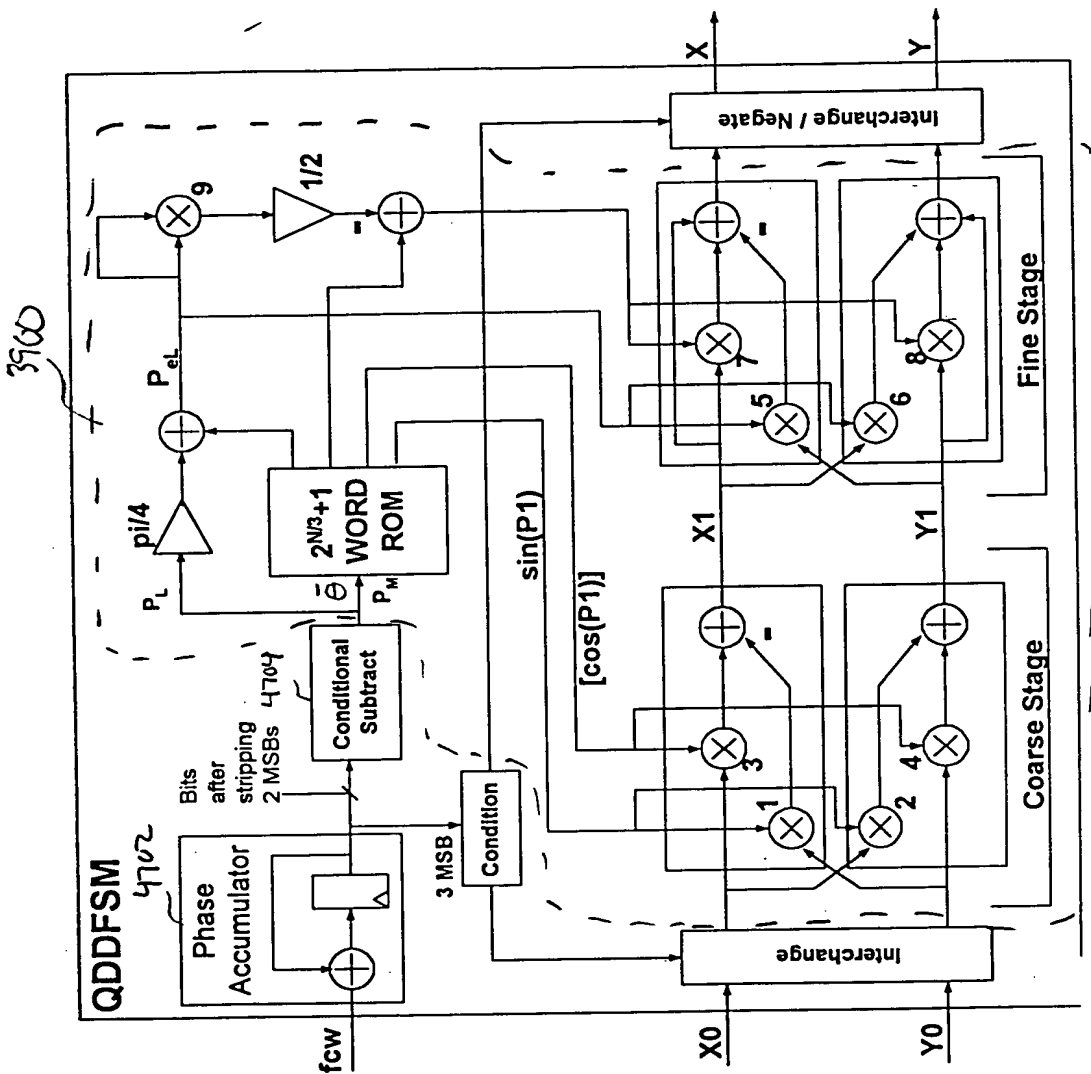


FIG 47

4000 →

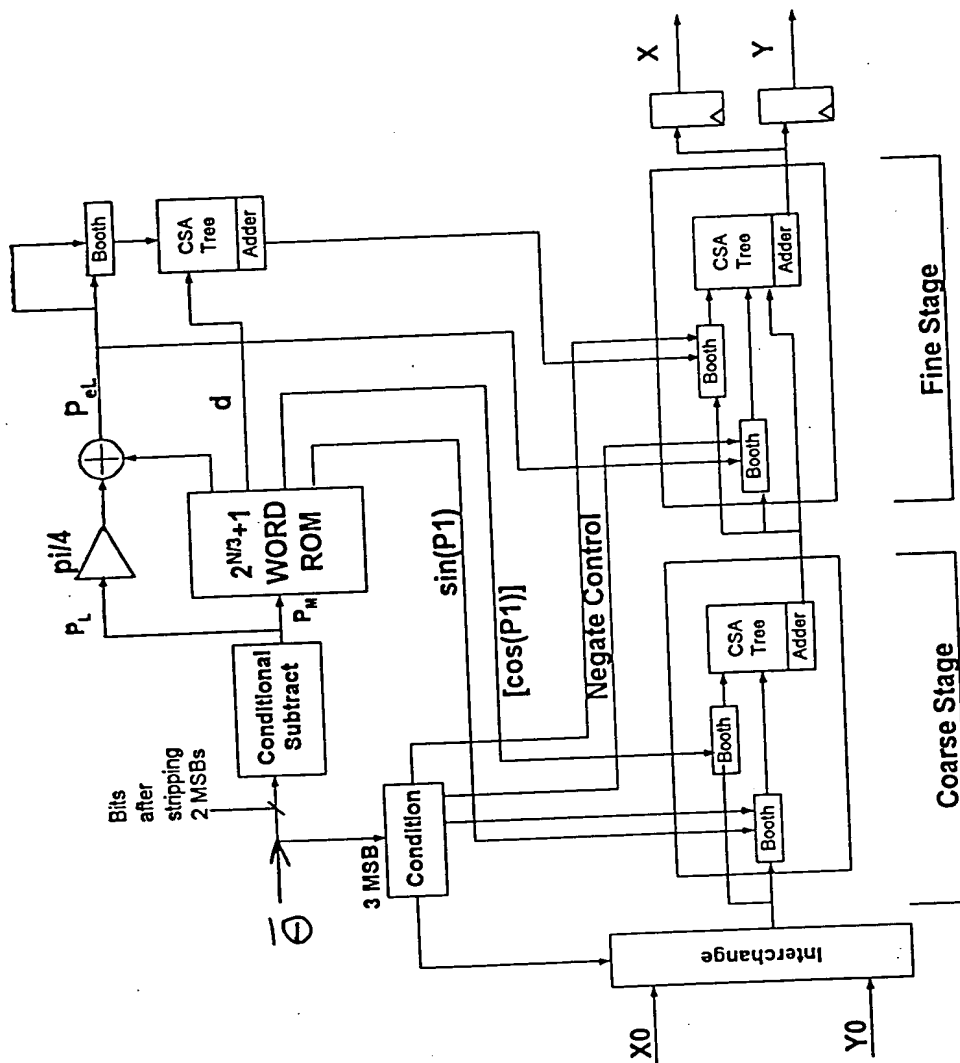


FIG. 48

000001 94286960

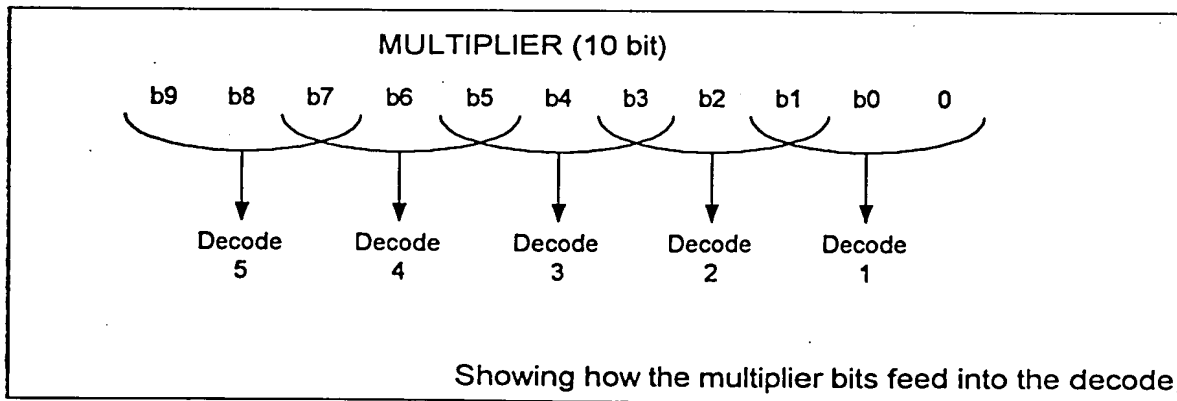
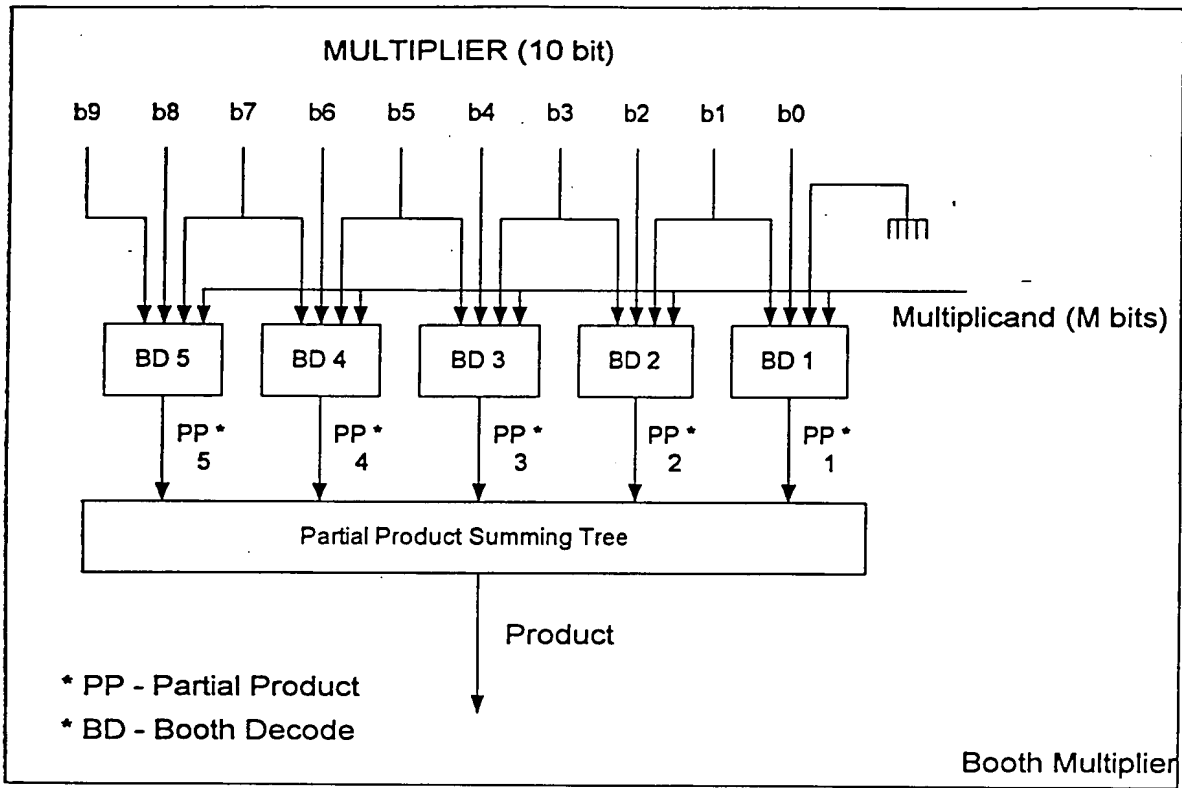


FIG. 49

5000  
↓

Original Booth Table

5002

b2 b1 b0 PP

0	0	0	0*A
0	0	1	1*A
0	1	0	1*A
0	1	1	2*A
1	0	0	-2*A
1	0	1	-1*A
1	1	0	-1*A
1	1	1	0*A

FIG. 50

5100  
↓

Negating Booth Table

5102

b2 b1 b0 PP

0	0	0	0*A
0	0	1	-1*A
0	1	0	-1*A
0	1	1	-2*A
1	0	0	2*A
1	0	1	1*A
1	1	0	1*A
1	1	1	0*A

FIG. 51



5260  
↓

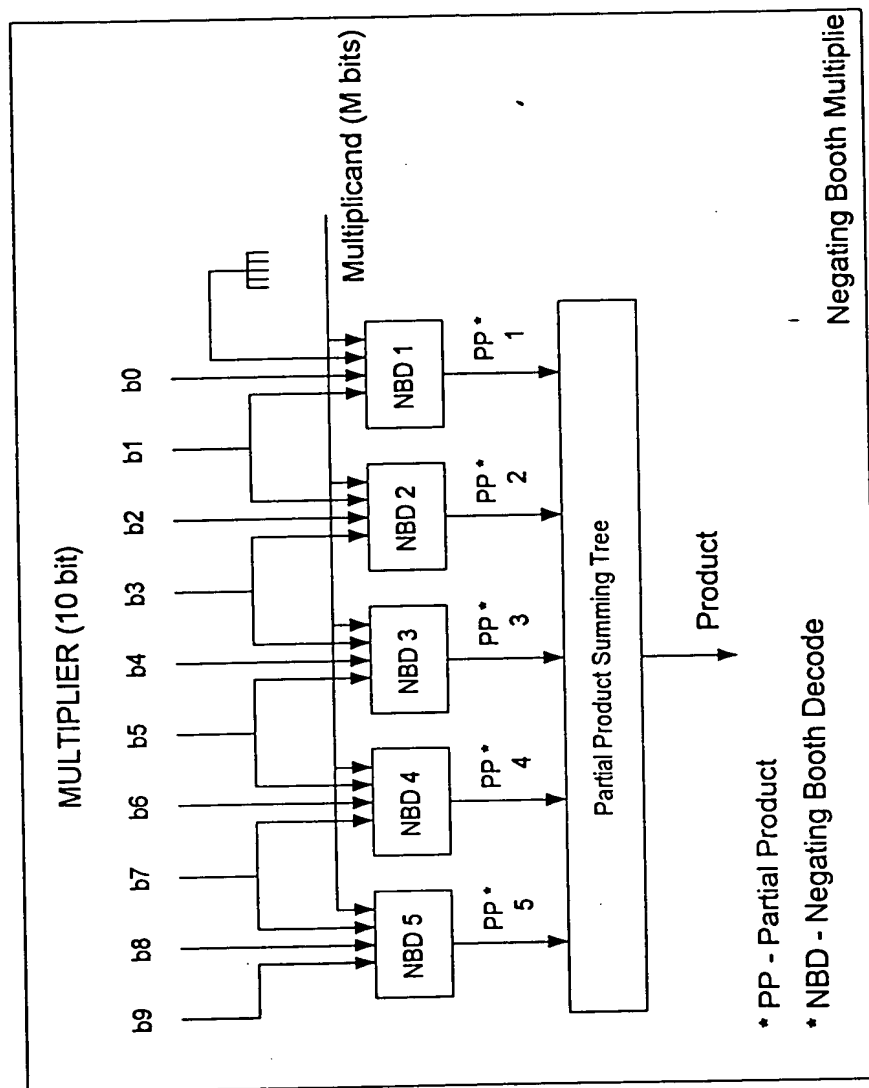


Fig. 52

5300

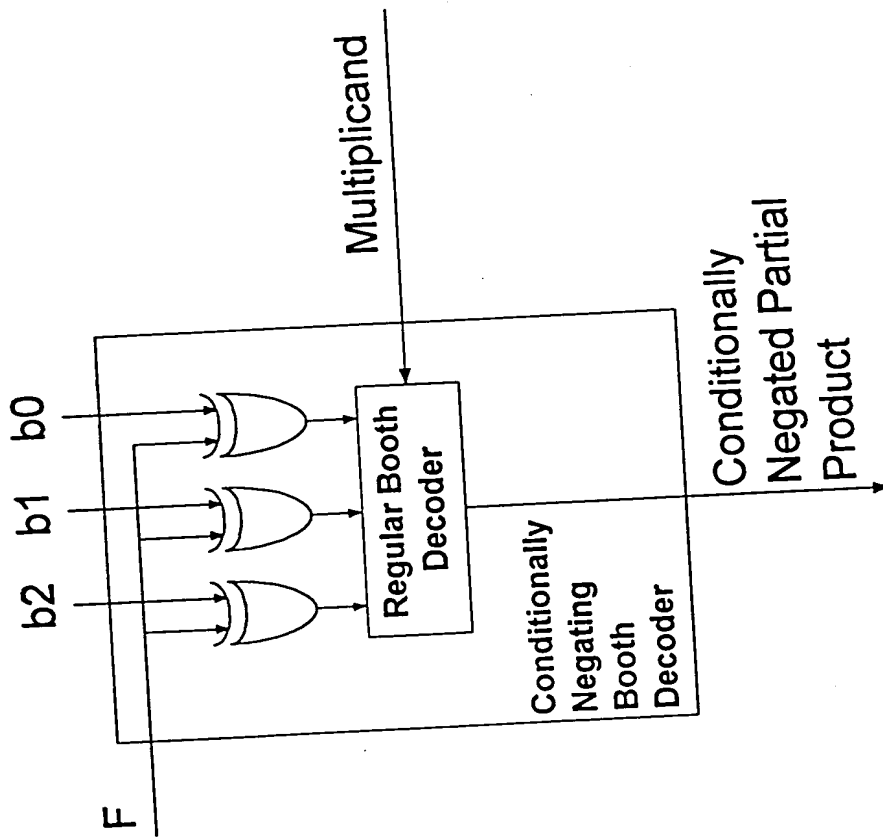


FIG. 53

5400

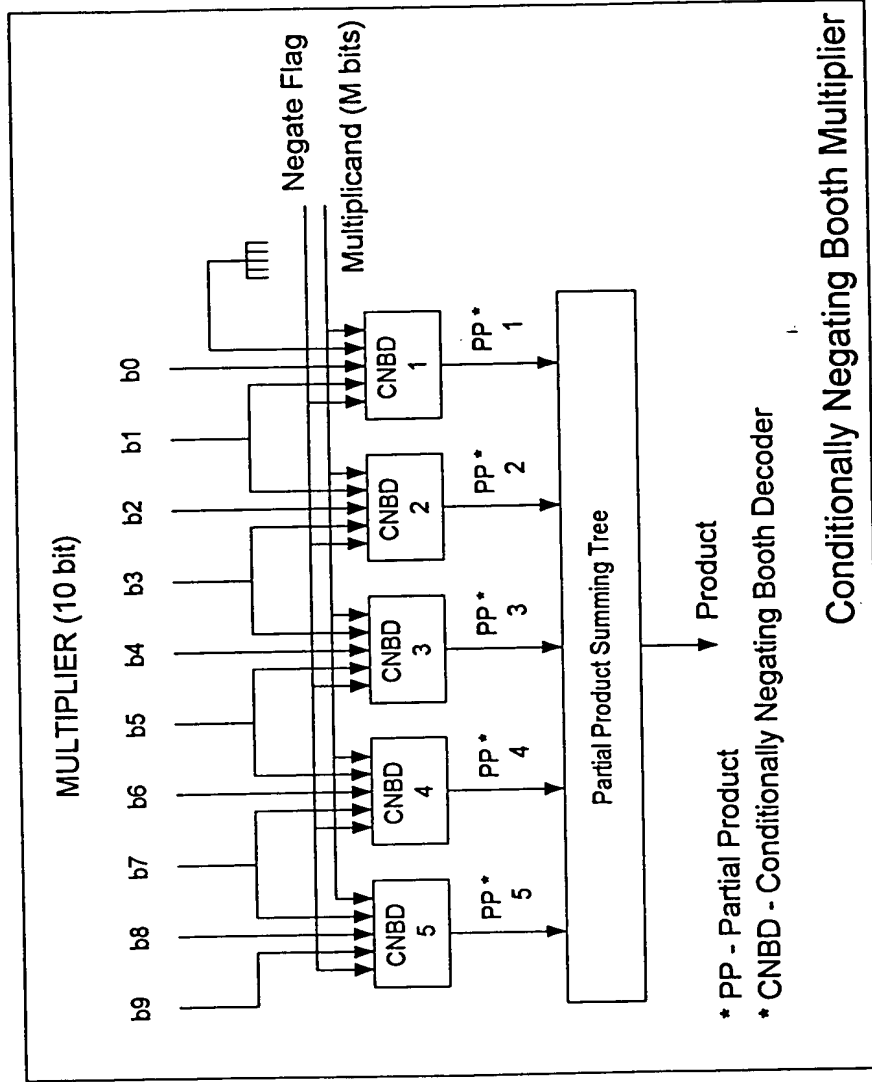


FIG. 54

5500

5502

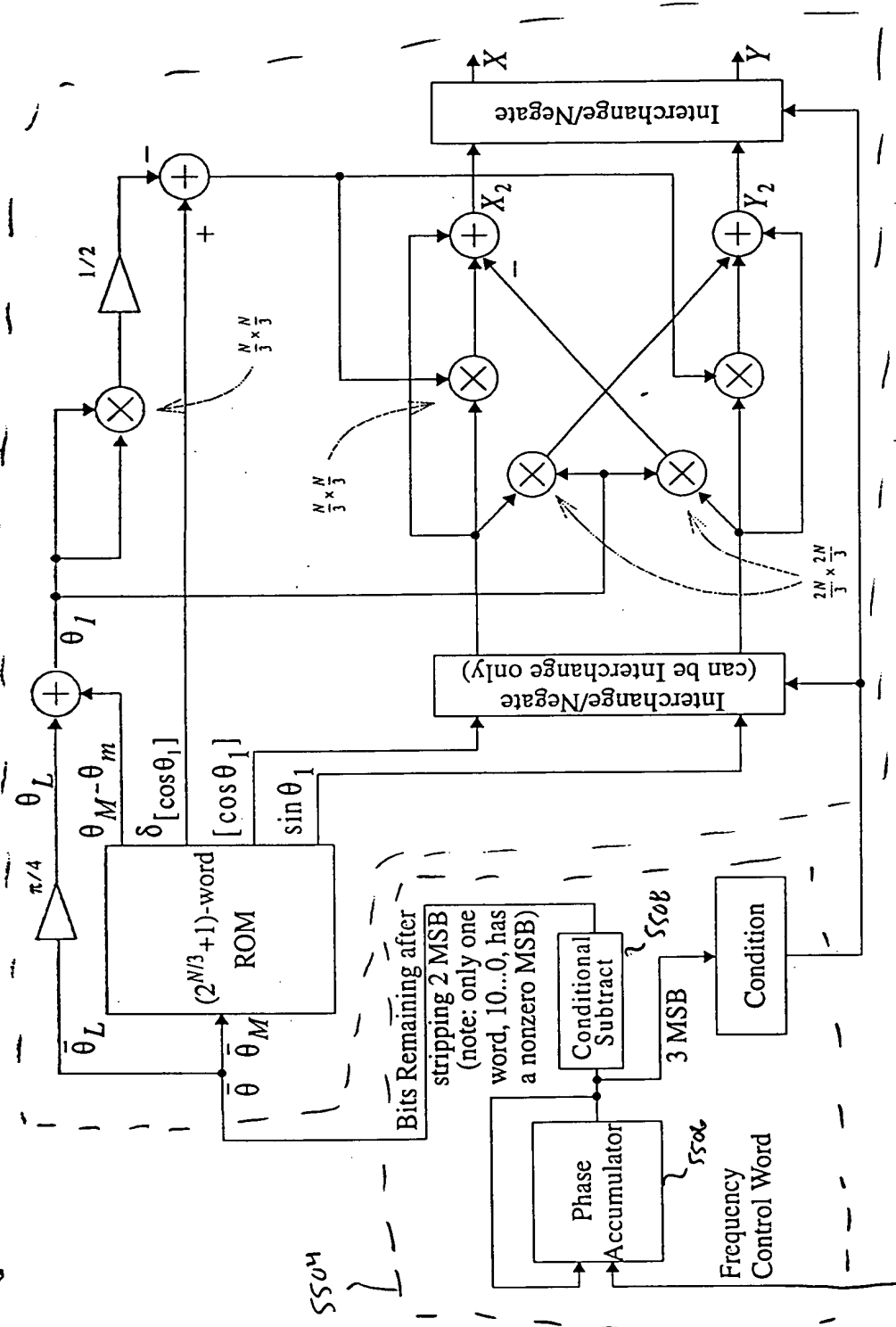


Fig. 55 Angle Rotator Configured as a Quadrature Direct Digital Synthesizer (QDDS).

5600

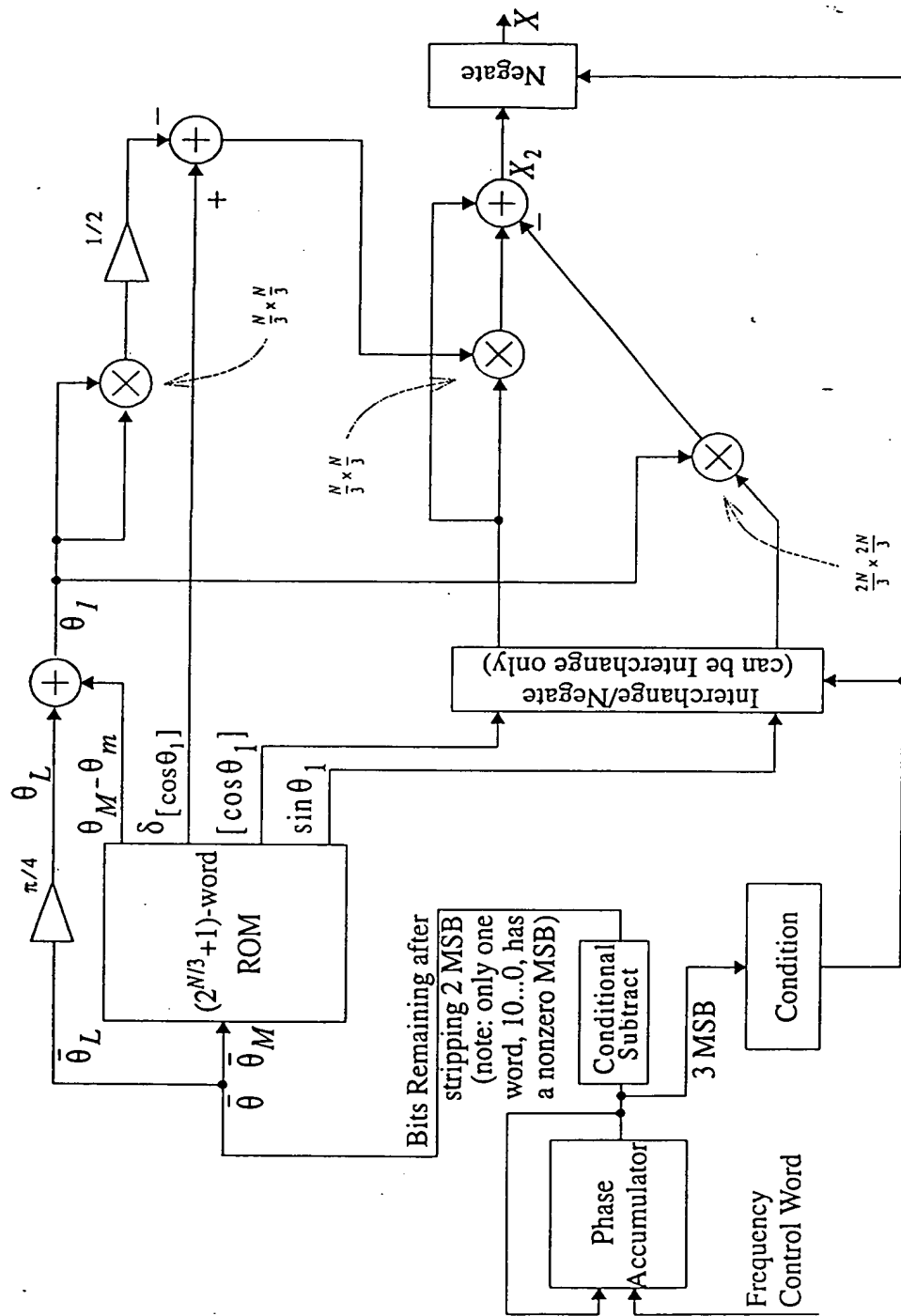


FIG. 56 Angle Rotator Configured as a "Cosine-only" Direct Digital Synthesizer (DDS) {from Fig 37}.

5700

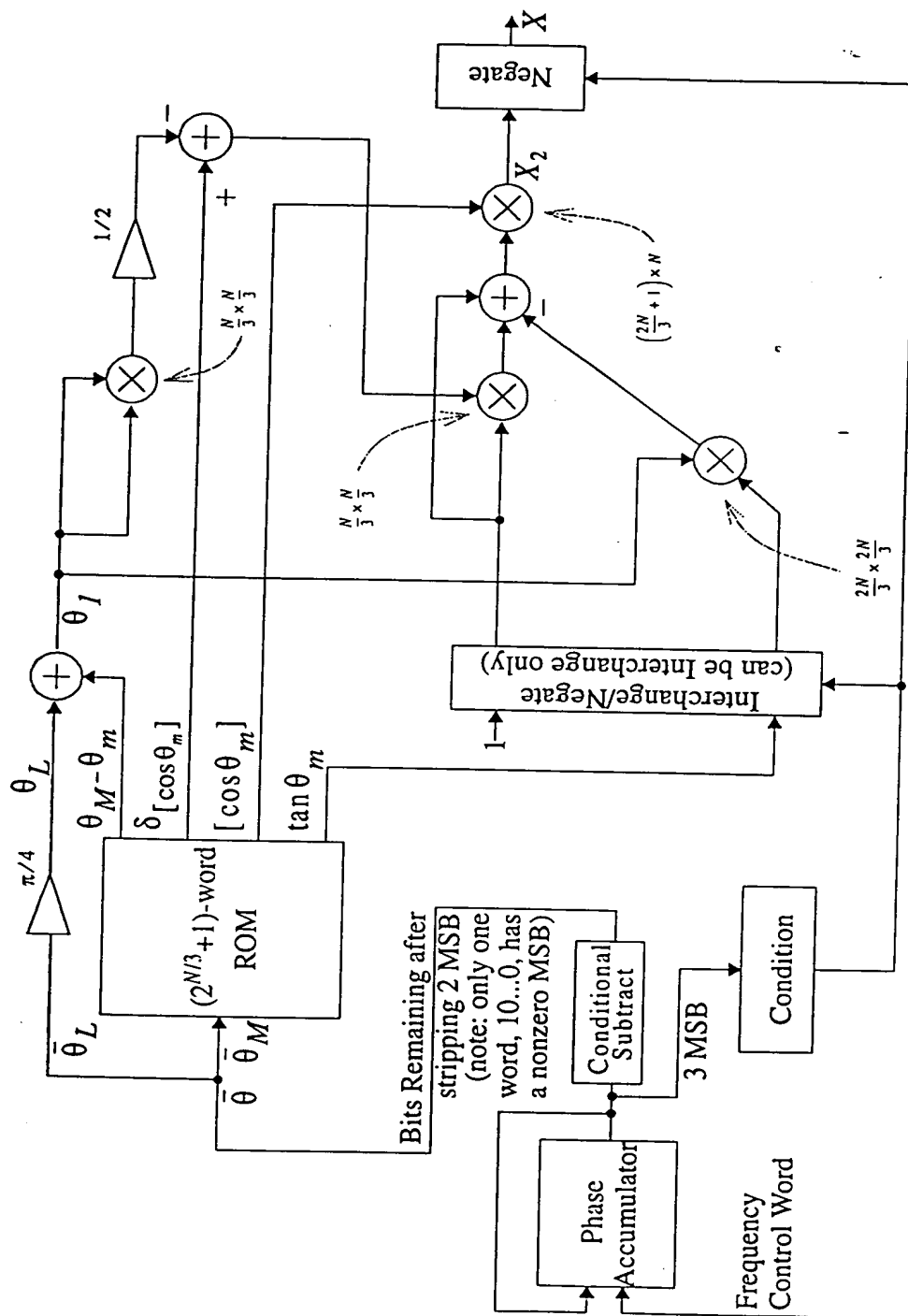


FIG. 57 Angle Rotator Configured as a "Cosine-only" Direct Digital Synthesizer (DDS) {from Fig. 44



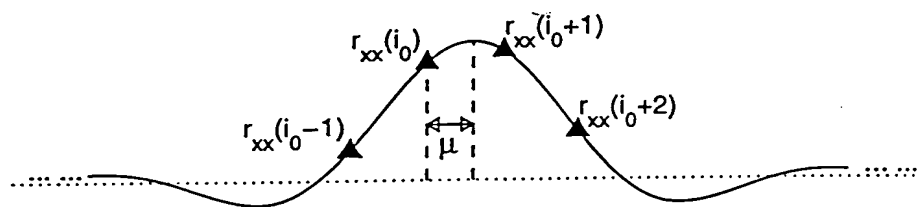


FIG. 60 Mean values of the preamble correlator output, for  $\theta = 0$ .

000001" 94286960



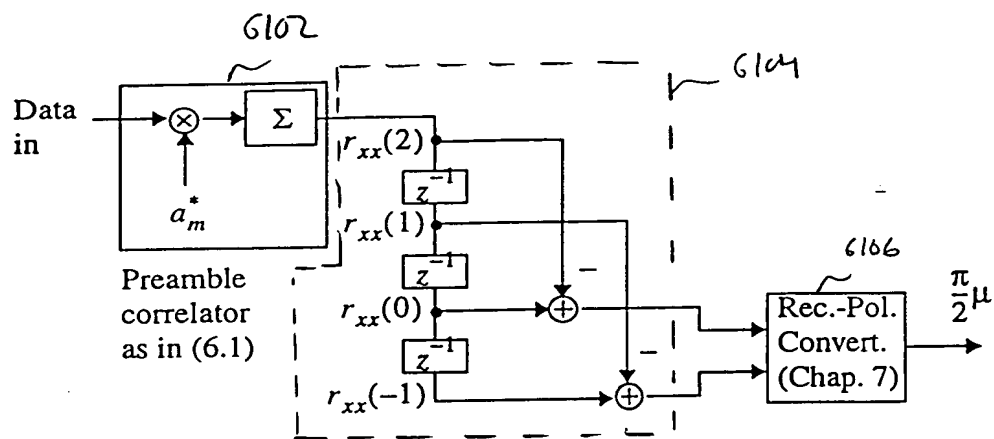


FIG. 612 Preliminary symbol-timing estimation structure.

[illegible]

GZCW

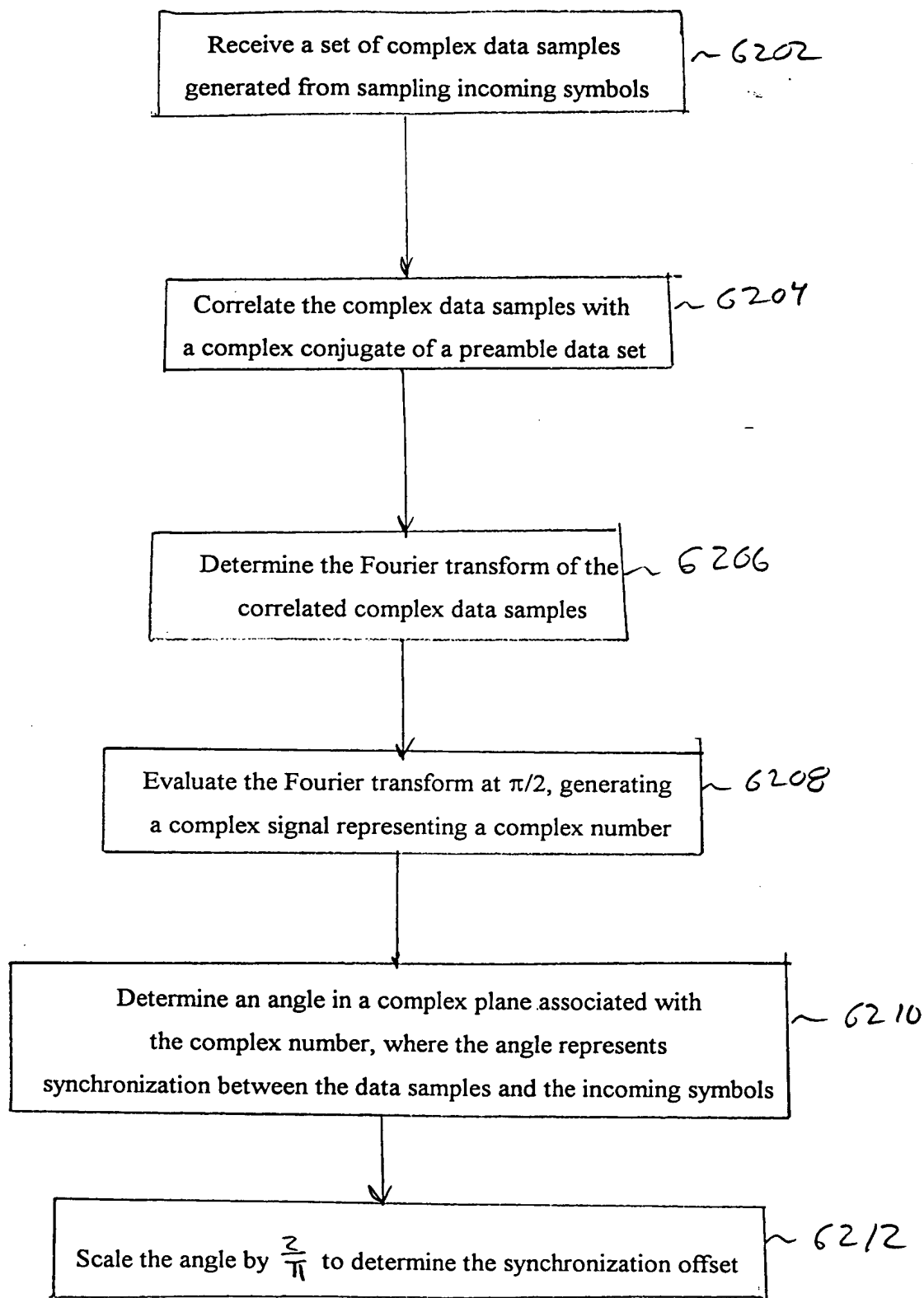


FIG. 62

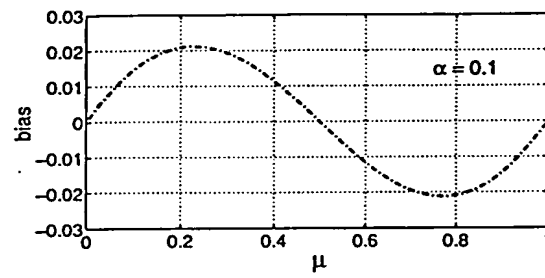


FIG. 63 Bias due to truncation.

6400

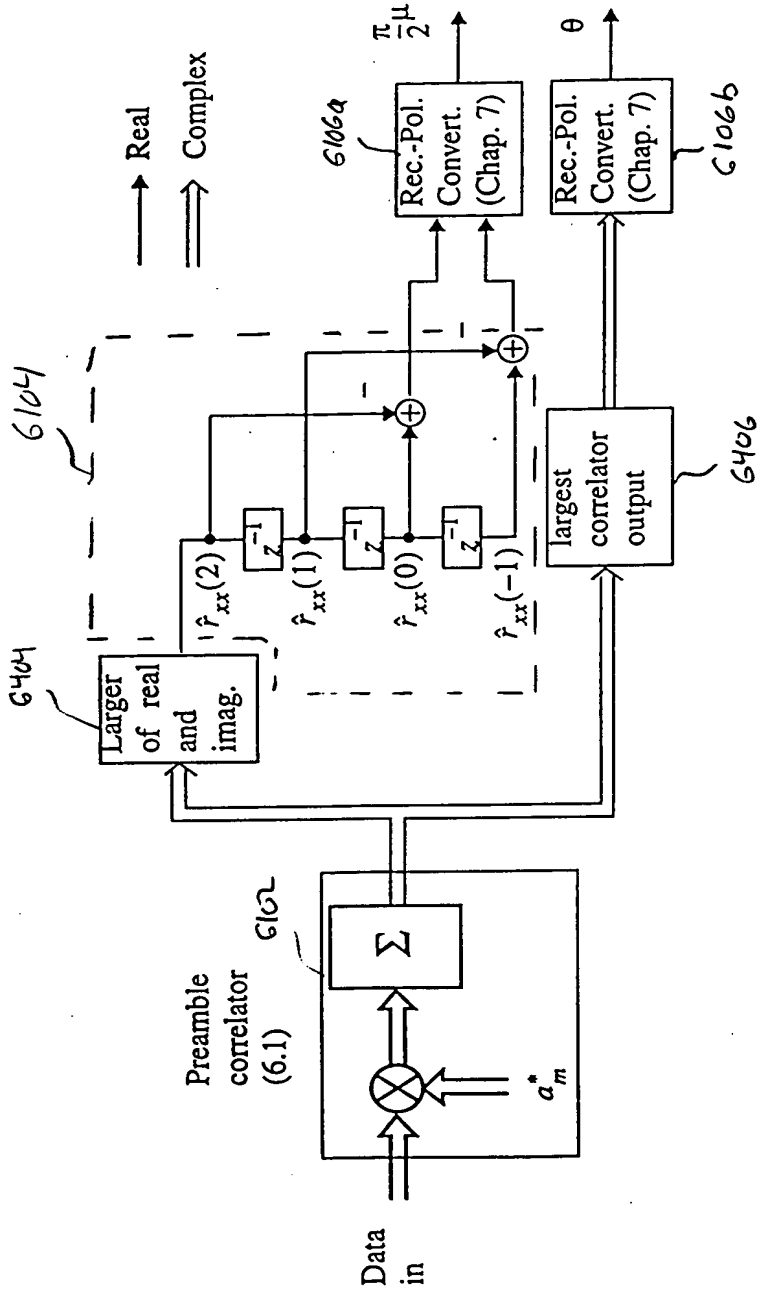


FIG. 64 Structure for carrier-phase and symbol timing recovery.

6500  
↓

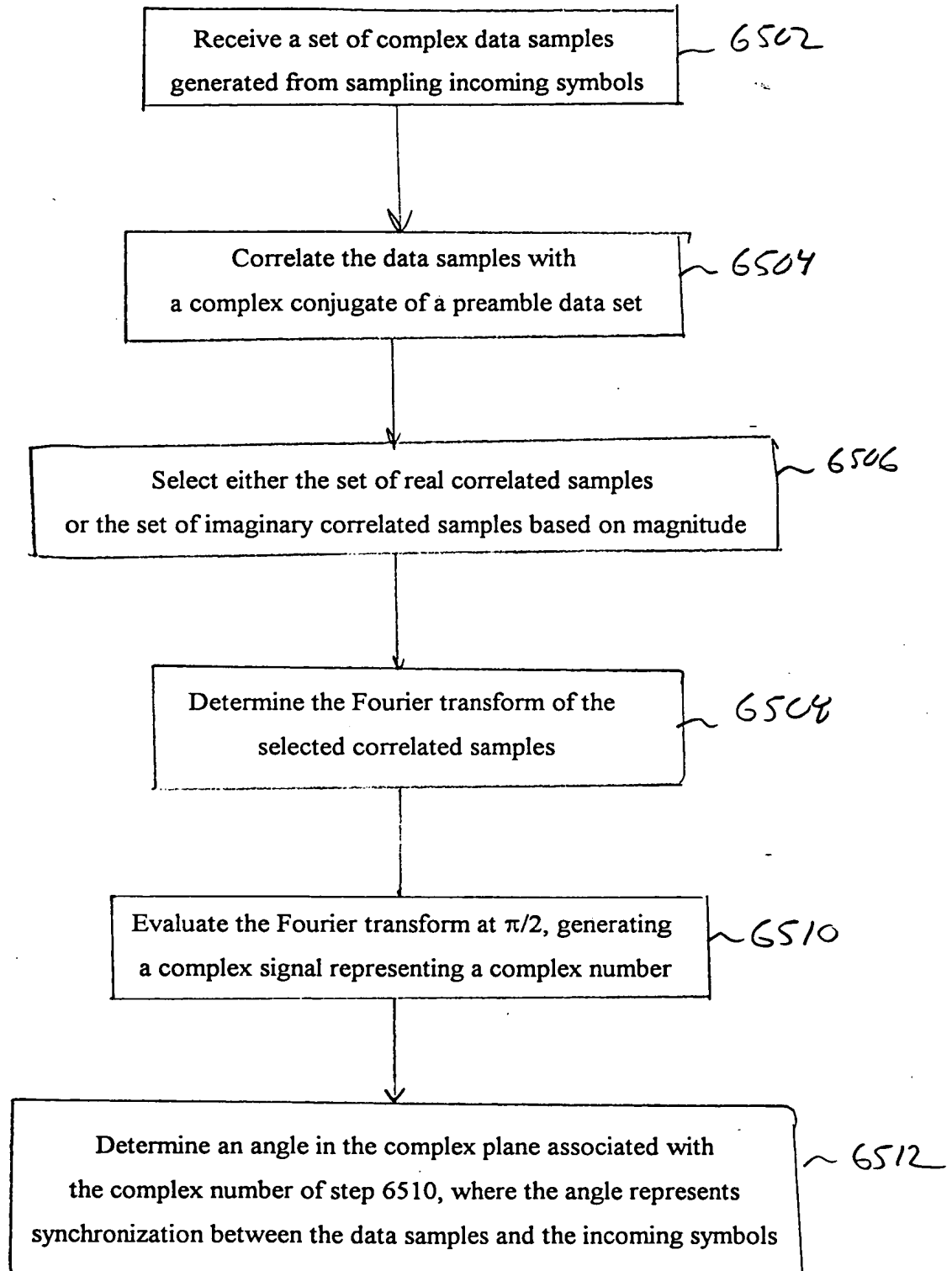


FIG. 65A

6500 (cont.)

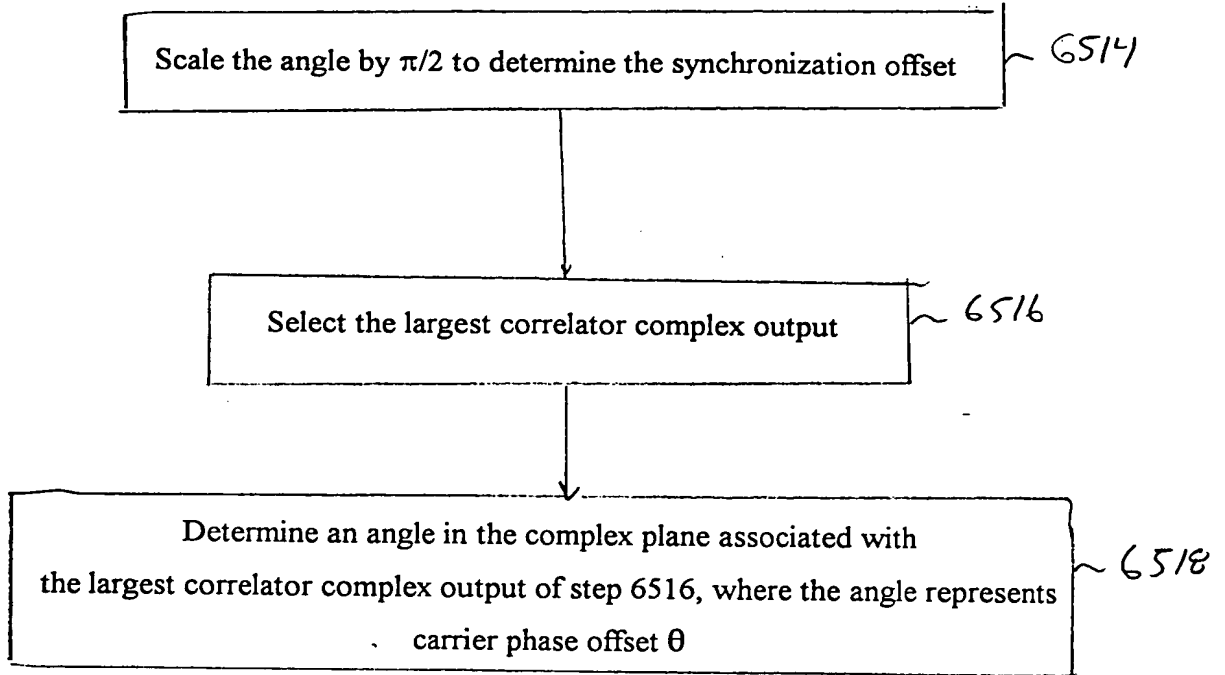


FIG. 65B

09698246 103000

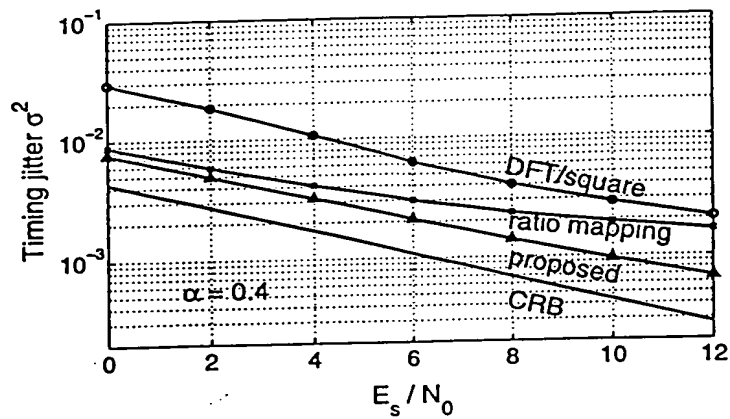


Figure 66: Timing jitter variance,  $\alpha = 0.4$ .

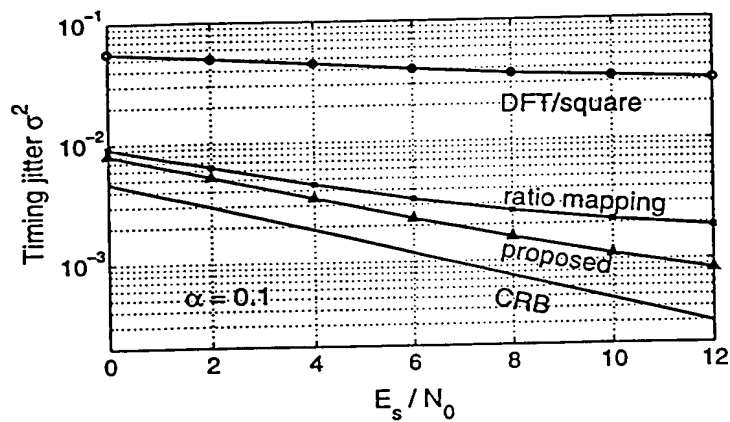


Figure 67: Timing jitter variance,  $\alpha = 0.1$ .

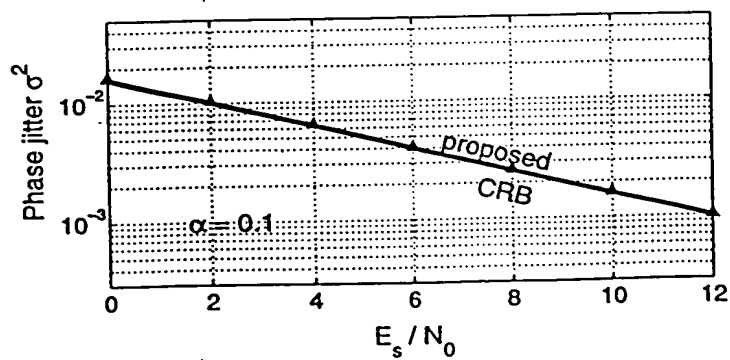


Figure 68: Phase jitter variance,  $\alpha = 0.1$ .

0968246-103000

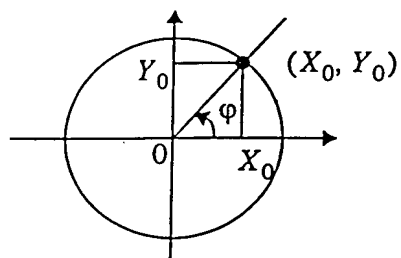
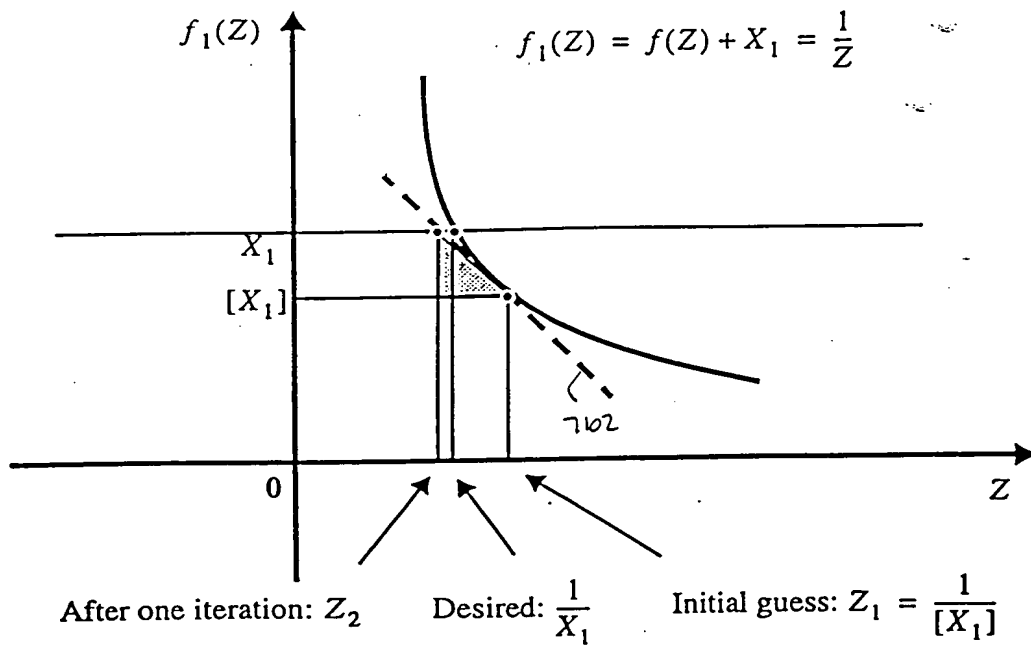
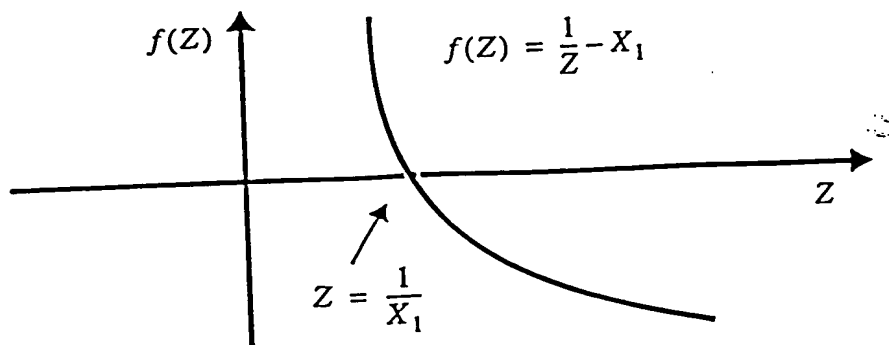


FIG. 69 Cartesian to polar conversion.





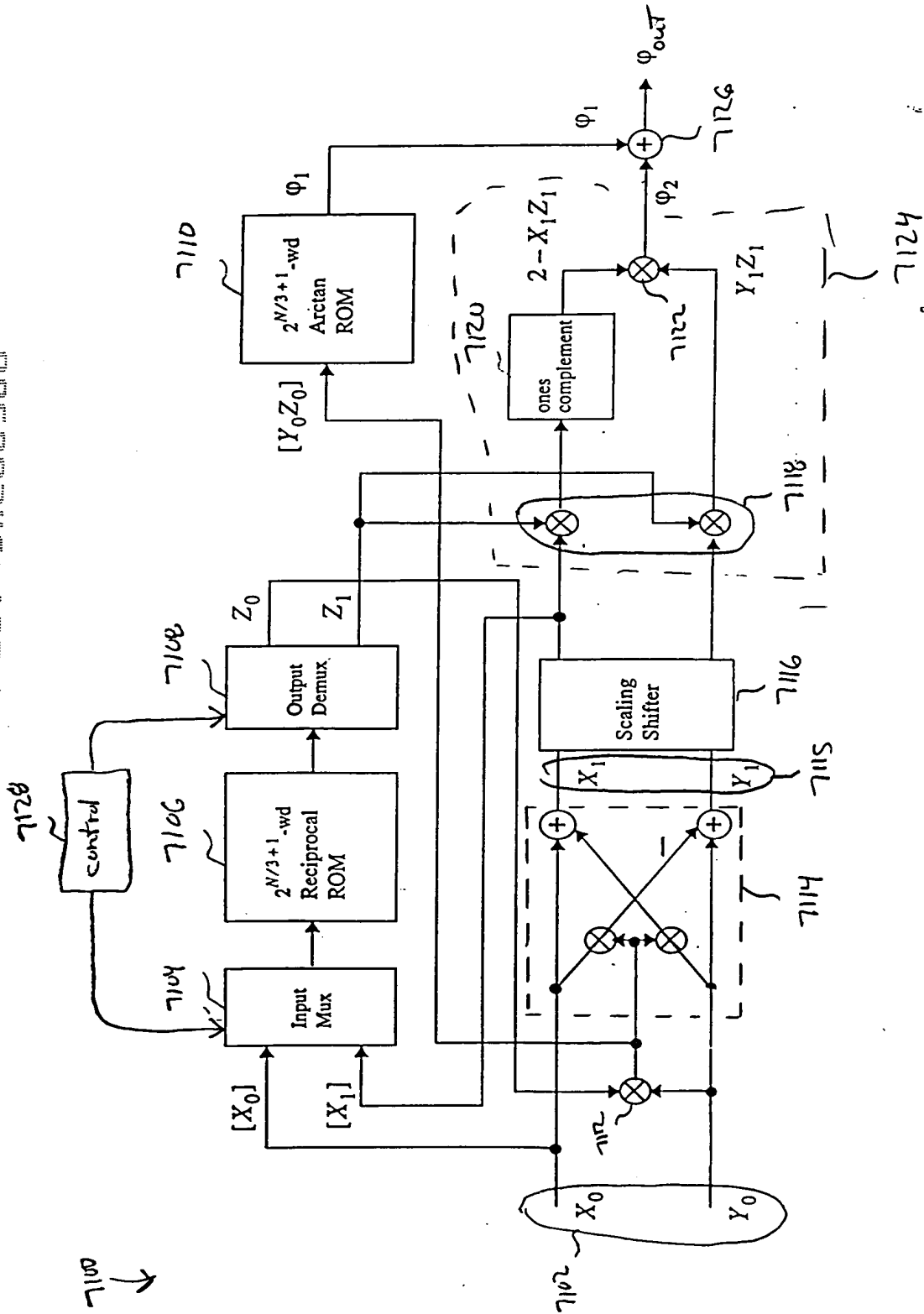


FIG. 71:

09698245 103000

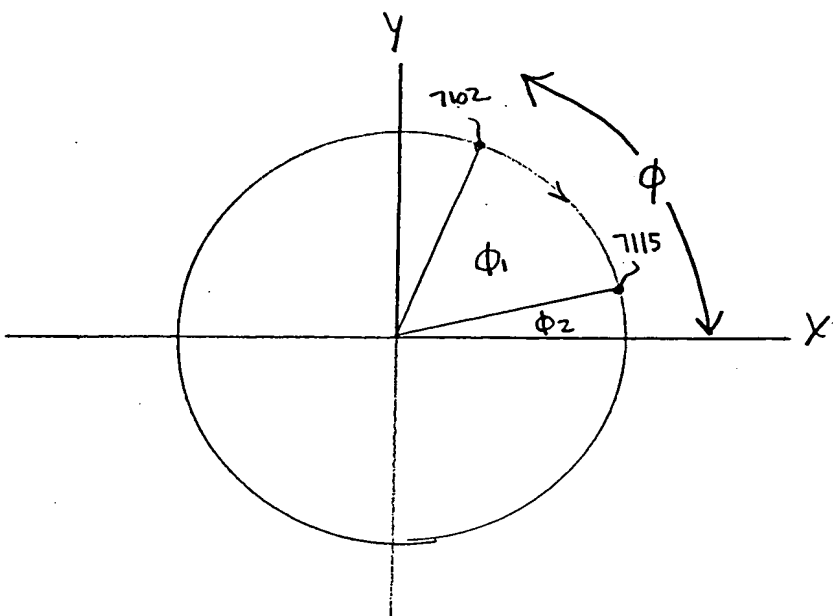


FIG. 72

7300  
↓

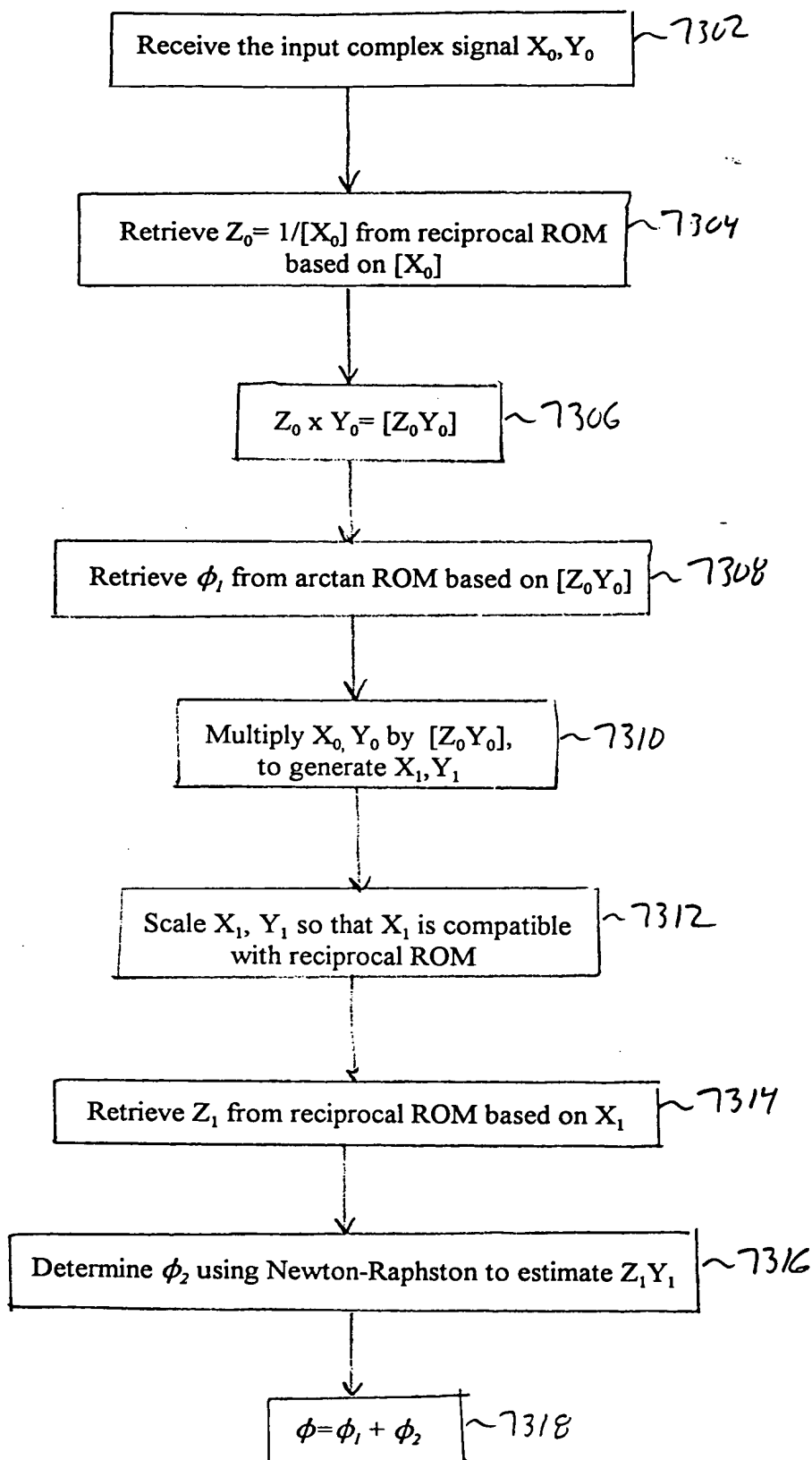


FIG. 73

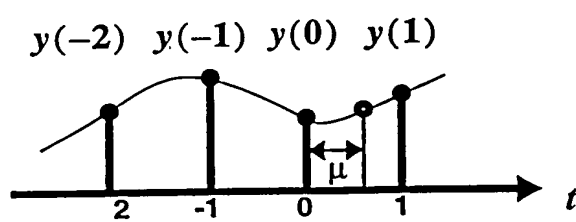


FIG. 74 Interpolation in a non-center interval.

FIG. 75A

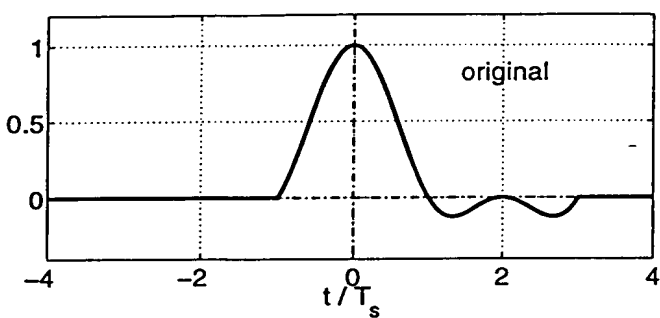


FIG 75B

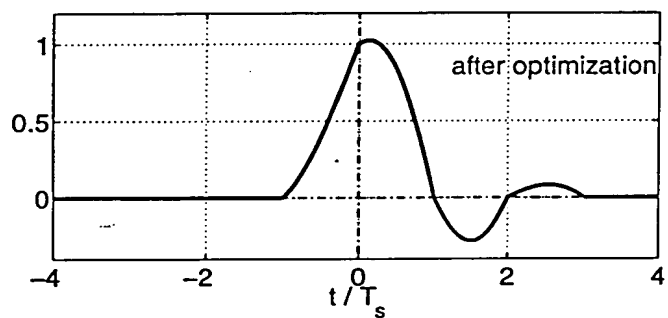


FIG. 75A-B: Impulse responses of the non-center-interval interpolation filter  $A$ , before and  $B$ , after optimization.

FIG. 76A

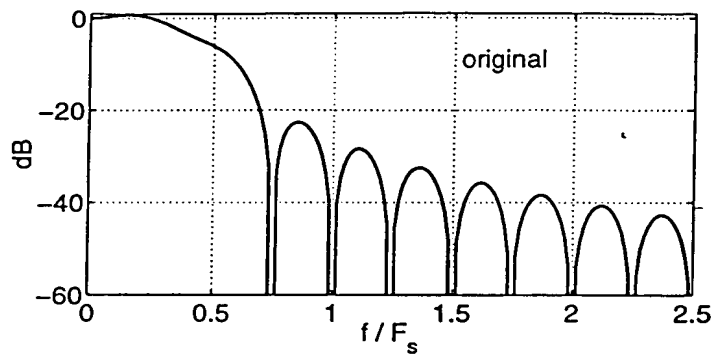


FIG. 76B

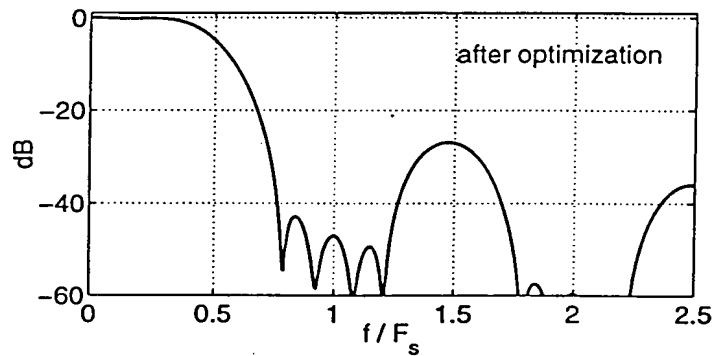


FIG. 76A-B : Frequency responses of the non-center-interval interpolator before optimization and , after optimization.

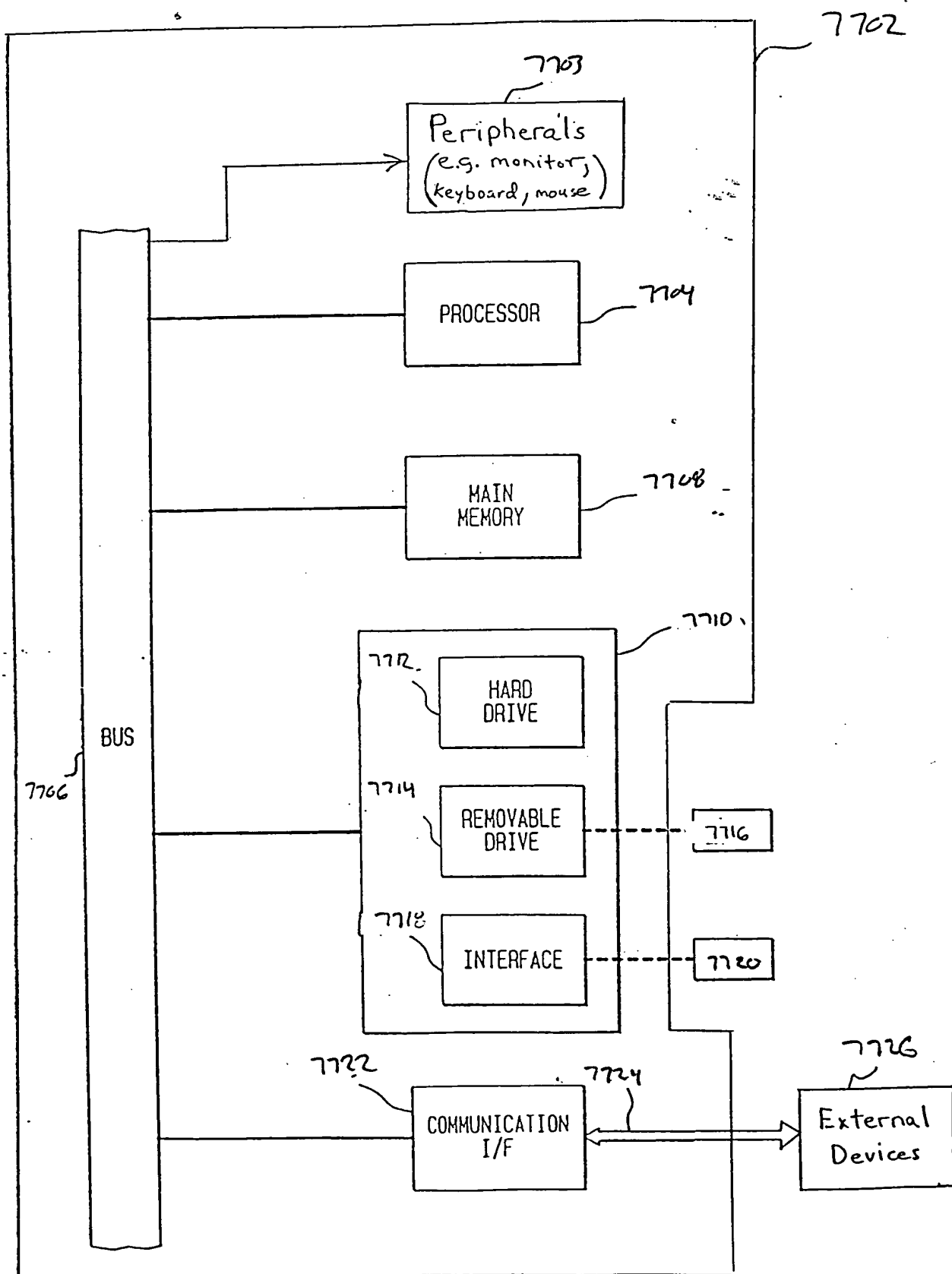


FIG. 77



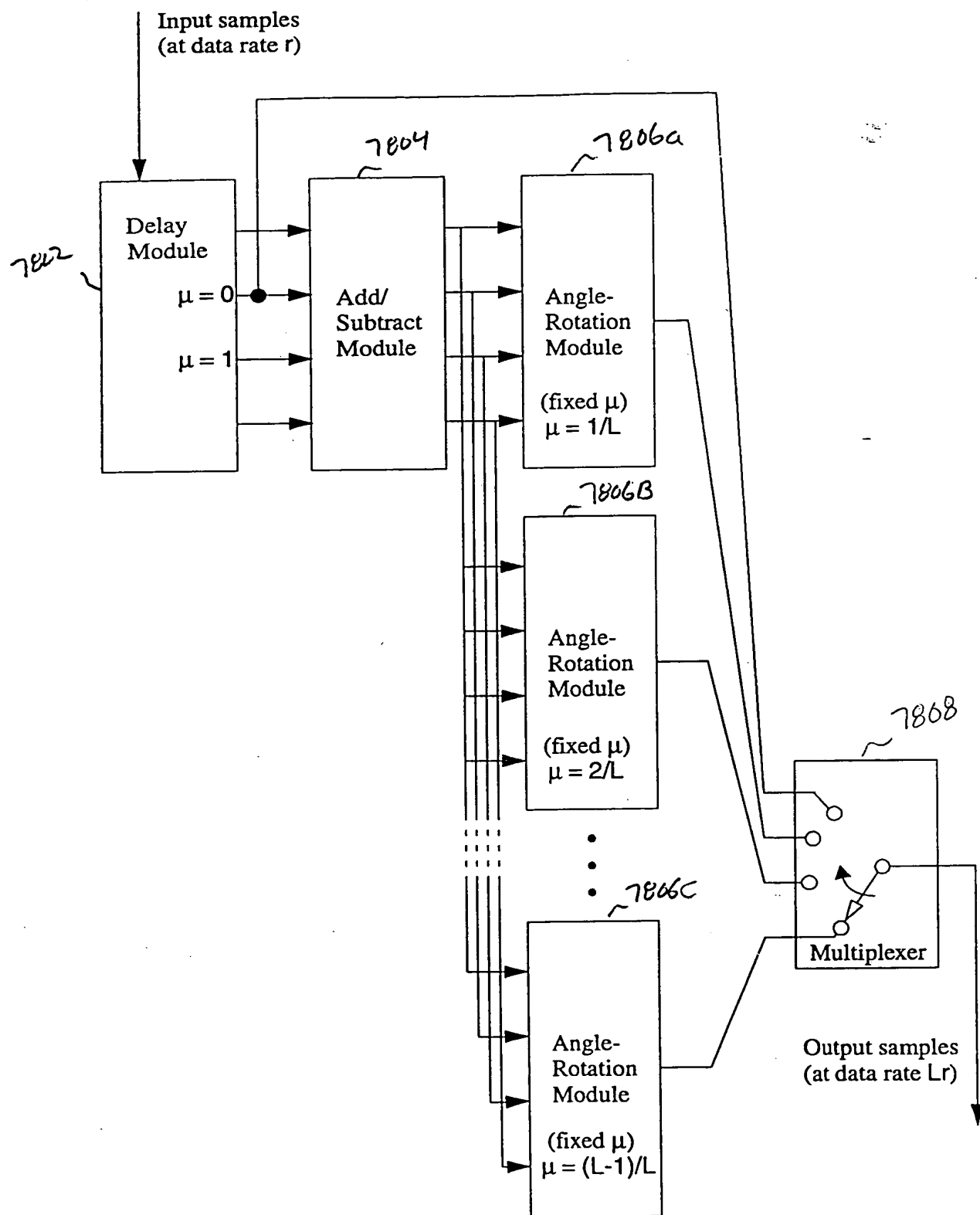


FIG. 78 Data Rate Expansion Circuit.

**This Page is Inserted by IFW Indexing and Scanning  
Operations and is not part of the Official Record**

## **BEST AVAILABLE IMAGES**

Defective images within this document are accurate representations of the original documents submitted by the applicant.

Defects in the images include but are not limited to the items checked:

- ☐ **BLACK BORDERS**
- ☐ **IMAGE CUT OFF AT TOP, BOTTOM OR SIDES**
- ☐ **FADED TEXT OR DRAWING**
- ☐ **BLURRED OR ILLEGIBLE TEXT OR DRAWING**
- ☐ **SKEWED/SLANTED IMAGES**
- ☐ **COLOR OR BLACK AND WHITE PHOTOGRAPHS**
- ☐ **GRAY SCALE DOCUMENTS**
- ☐ **LINES OR MARKS ON ORIGINAL DOCUMENT**
- ☐ **REFERENCE(S) OR EXHIBIT(S) SUBMITTED ARE POOR QUALITY**
- ☐ **OTHER:** \_\_\_\_\_

**IMAGES ARE BEST AVAILABLE COPY.**

**As rescanning these documents will not correct the image problems checked, please do not report these problems to the IFW Image Problem Mailbox.**